AUSTRIAN
MARSHALL PLAN FOUNDATION
VIENNA | AUSTRIA

Marshall Plan Scholarship Report

Parkinson's Assistive Technology

Lukas Bernhofer

Supervised by

UNIVERSITY
OF APPLIED SCIENCES
UPPER AUSTRIA

University of Portland

Fh-Prof. Dipl.-Ing.
Reinhard Gahleitner

Assoc. Prof. Dr.
Timothy Doughty

January 2016

Contents

1 Introduction

The topic of this work was selected in relation to an exchange program with the University of Portland (UP) in Portland, Oregon. The duration of this program was set up for one semester covering the time from 31st of August 2015 to the 18th of December 2015.

The National Academy of Engineering has identified grand challenges for engineers in the 21st century and the University of Portland has picked one of these challenges, engineering better medicines, to focus on. Addressing this, the University of Portland's mechanical engineering professor Dr. Timothy Doughty has collaborated with students to create tools to help Parkinson's patients.[5]
Dr. Doughty began his research in fall 2005, and this research was first brought in connection with students in the form of a senior design project in fall 2008. Since then, the research work has continued to involve the students with senior design projects on this topic.
The research of Dr. Timothy Doughty focuses on tremor, the mechanical point of view of the Parkinson's disease. To tackle theses issues, there is ongoing work of designing walking equipment to decrease tipping hazard and eating utensils to reduce hand tremors.[5]

The topic of Parkinson's disease is also relevant to the Marshall Plan Scholarship, as this disease is an issue in Austria as well as in the United States and it is not just limited to these two countries, it is a worldwide problem. According to the Parkinson's Disease Foundation, an estimated amount of seven to 10 million people worldwide are living with this disease.[6]

2 Abstract

Ongoing research for curing Parkinson's disease focuses on the neurological aspect of the disease in order to heal it with medication and surgery. This work solely emphasizes the mechanical aspect of the disease, the tremor, which is visible to the environment. More precisely, the goal is to develop a wearable device to tackle the target symptom, which is the tremor produced around the axis built by the forearm of the human being.

Analyzing tremor data and searching for excited frequencies is the origin for the development of a device that counteracts the produced vibrations. A One Degree of Freedom differential equation model of a person's forearm describes the motion, where the model's input is due to the actuation of the biomechanics of the human being's arm.
Modeling the wearable device together with the arm using a linear differential equation system makes it possible to calculate a Frequency Response Function of the system composed of two parts. There is a fixed contribution from the arm and an adjustable part form the wearable device.
Data of a human's arm are used for the theory model as well as for a testing setup that simulates a Parkinson's patient's shaking. This setup constitutes a reproducible, adaptable and readily available testing environment.

Based on the linear differential equation system, the required parameters for the wearable device are evaluated. The arm/wearable device system is tuned so that the vibrations are absorbed around the mainly excited frequencies of a Parkinson's patient's tremor.

3 About Parkinson's disease

3.1 Definition and Causes

"Parkinson's disease is a progressive disorder of the nervous system that affects movement. It develops gradually, sometimes starting with a barely noticeable tremor in just one hand. But while a tremor may be the most well-known sign of Parkinson's disease, the disorder also commonly causes stiffness or slowing of movement."[7]

A common abbreviation for Parkinson's disease is PD and therefore may be used in this document.

According to Parkinson's Disease Foundation, about seven to 10 million people worldwide are living with Parkinson's disease. In America alone, as many as one million people live with PD and approximately 60,000 are diagnosed with this disease each year, not reflecting thousands of cases that go undetected. In general, men are one and a half times more likely to have Parkinson's than women, which is also evident from Figure (1). According to the Parkinson's Disease Foundation, the combined direct and indirect cost of Parkinson's, including treatment, social security payments and lost income from inability to work, is estimated to be nearly 25 billion dollars per year in the United States alone. Compare [6] for previous chapter.

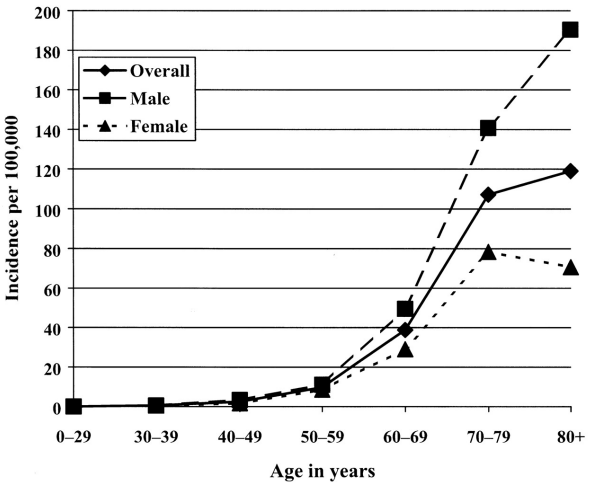

Figure 1: Incidence by age and gender[8]

Famous people suffering from Parkinson's Disease include Bhumibol Adulyadej, Muhammad Ali and Michael J. Fox. The latter founded The Michael J. Fox Foundation, which is dedicated to finding a cure for Parkinson's disease.

Parkinson's disease was first described by an English doctor, James Parkinson, in 1817. Today, Parkinson's disease is characterized as a disorder of the central nervous system that results from the loss of cells in the substantia nigra, see Figure (2), a region of the brain producing dopamine which is a chemical messenger responsible for transmitting signals for coordination of movement. Reduction of dopamine causes neurons to fire without normal control, and therefore people suffering from Parkinson's disease are less able to direct or control their movements. Compare [9] for previous chapter.

Figure (3) shows dopamine innervation assessed by 18-fluorodopa positron emission tomography (PET), whereby scan A depicts a control subject showing high striatal uptake (highest value in red) and scan B depicts an example of a patient with Parkinson's disease with motor signs mainly confined to the left limbs.[10]

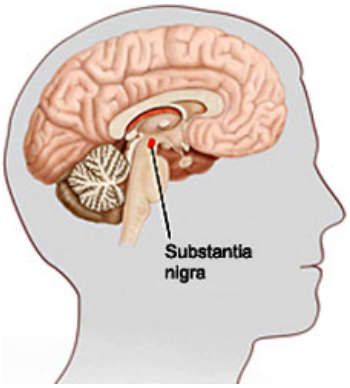

Figure 2: Substantia nigra[11]

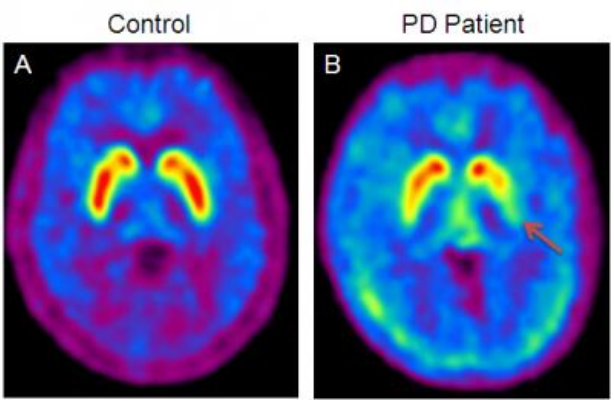

Figure 3: PET scan of two brains[10]

Although the exact cause of Parkinson's disease is unknown, research points to a combination of genetic and environmental factors.[9]

3.1.1 Genetic causes[12]

As the source [12] is mentioned in the headline, it is applicable for the whole Section (3.1.1). According to this source the majority of Parkinson's cases are not directly inherited, even though the cause is called genetic. About 15 to 25 percent of people reported to have Parkinson's have a relative with the disease. Studies have shown that people with a first-degree

relative suffering from PD, such as parent or sibling, have a four to nine percent higher chance of developing PD. Researchers have found several gene mutations that may cause Parkinson's disease directly. Some of these that play a role in dopamine cell functions are PINK1, LRRK2, DJ-1, and glucocerebrosidase, among others. Despite the rare incidence of genetic forms of PD, genetics is currently the subject of intense research because these forms of a disease can be studied in great detail in the laboratory.

3.1.2 Environmental causes[12]

Some scientists have researched that Parkinson's disease may result from exposure to an environmental toxin or injury including factors such as rural living, well water, manganese and pesticides. Studies have shown that occupational exposure to certain chemicals present in insecticides, including permethrin, the beta-hexachlorocyclohexane (beta-HCH) and the fungicide maneb, also elevate the risk of suffering from Parkinson's disease. Another toxin which can cause parkinsonism is the neurotoxin MPTP which was discovered by individuals who injected themselves with a synthetic form of heroin contaminated with MPTP. Although these factors are researched, there is no conclusive evidence that any environmental factor alone can be considered a cause of Parkinson's disease.

3.2 Symptoms[1]

The symptoms of Parkinson's disease can be categorized as Primary Motor Symptoms, Secondary Motor Symptoms and Nonmotor Symptoms, but every person with Parkinson's will experience these symptoms differently.

By definition, Parkinson's is a progressive disease which can be observed in patients who first have symptoms only on one side of the body. After many years, these symptoms eventually begin on the other side, but often do not become as severe as symptoms on the initial side. The subsequent section deals with the different categories of the symptoms mentioned above.

3.2.1 Primary Motor Symptoms

The diagnosis of Parkinson's is not based on a test. Instead, it requires a careful medical history and a physical examination to detect the signs of the disease by observing the Primary Motor Symptoms. Four of these symptoms are Resting Tremor, Bradykinesia, Rigidity and Postural Instability which are described as follows.

Resting Tremor
This tremor consists of a shaking or oscillating movement and usually appears when the muscles are relaxed or at rest, which is the reason for the name of this type of tremor. These tremors mostly start mildly in the finger, hand and foot on one side of the body. This type of tremor usually ceases when the person begins performing actions, and so some PD patients have noticed that they can stop a hand tremor by keeping the hand in motion. The Resting Tremor can be amplified by stress or excitement. As the disease is progressive, the tremor often spreads to the other side of the body but mostly stays stronger on the initially affected side. This symptom, the Resting Tremor, is the most noticeable outward sign of Parkinson's disease.

Bradykinesia
Bradykinesia means "slow movement," and related to Parkinson's disease it describes a general reduction of spontaneous movement. It can give the appearance of stillness, cause a decrease in facial expressivity and affect a person's speech as the speech becomes quieter and less distinct. Bradykinesia can also cause difficulties while walking because affected persons may walk with short, shuffling steps.

Rigidity
Rigidity causes stiffness of the limbs, neck and trunk. It is induced because a PD patient's muscles don't relax at rest as usual, and so the muscle tone of an affected limb is always stiff. A person with Rigidity and Bradykinesia tends to stop swinging the arms when walking. In addition to being uncomfortable, Rigidity can even be painful in the worst case.

Postural Instability

Postural Instability is a tendency to be unstable when standing upright due to the loss of some of the reflexes needed for staying in an upright position. The consequence is that patients with Postural Instability may topple backwards if they are jostled slightly. Therefore a common test to diagnose this symptom of PD is giving the patient a moderately forceful backwards tug while standing and observing how well the person recovers. This method is called pull test.
Postural Instability can also cause difficulties when pivoting, making turns, performing quick movements or even when rising up from a chair.

3.2.2 Secondary Motor Symptoms

The best known Secondary Motor Symptoms are Freezing, Micrographia, Mask-like Expression and Unwanted Accelerations. However, there exist many others such as stooped posture which is the tendency to lean forward, dystonia, impaired fine motor skills, gross motor dexterity, difficulty swallowing, cramping and drooling.

Freezing

Freezing of gait is different than Rigidity and Bradykinesia because it is when people hesitate before stepping forward and feel like their feet are glued to the floor. However, if the patient gets past the first step, often the person can enter a normal stride.
Various types of attempts, such as an exaggerated first step, can help, but some individuals have severe freezing in which they simply cannot take a step. Freezing is also a problem because it increases a Parkinson's disease patient's risk of falling forward.

Micrographia

Micrographia describes the shrinkage in handwriting that progresses the more a person with PD writes and is a result of Bradykinesia.

Mask-like Expression

This phenomenon describes when a Parkinson's patient's face may appear

less expressive due to decreased unconscious facial movements. It may result from a combination of Rigidity and Bradykinesia.

Unwanted Accelerations
Whereas the symptoms above described only a decrease in the speed of movement, there is also the possibility of an increase. Nevertheless, this fact can cause troubles in speech and movement and potentially increase the risk for falls.

3.2.3 Nonmotor Symptoms

Nonmotor Symptoms do not involve movement, coordination, physical tasks or mobility and are way more difficult to deal with because of their invisibility to other people in the patient's surroundings.
The best known Nonmotor Symptoms are loss of sense of smell, constipation, sleep disorder, mood disorder and orthostatic hypotension. According to researchers, they may precede motor symptoms by years.
Further Nonmotor Symptoms include bladder problems, excessive saliva, weight loss or gain, sexual problems, depression, anxiety and loss of energy. Cognitive issues involve memory difficulties, slowed thinking, confusion and, in some cases, dementia.

3.3 Treatments

Up to now, the cause of Parkinson's disease is unknown and therefore scientists have not yet found a way to cure this disease. However, the approach is to treat the symptoms rather then the disease on its own. There are many medications available to treat the symptoms of Parkinson's, and there are also options for surgical treatments. Compare [13] for previous chapter.

3.3.1 Medications[13]

Each person with Parkinson's must be individually evaluated to determine which drug or combination of drugs is best for them, because drug

treatment depends on many factors including symptom presentation, other concurrent health issues and the patient's age.

Carbidopa/Levodopa

According to the Parkinson's Disease Foundation, Carbidopa/Levodopa remains the most effective drug for treating PD. Adding carbidopa prevents levodopa from being converted into dopamine in the bloodstream, allowing more of it to get to the brain which reduces the needed amount of levodopa for treating symptoms. Patients experience side effects such as spontaneous, involuntary movements and on-off periods when the medication will suddenly and unpredictably start or stop working.

Dopamine agonists

Dopamine agonists are drugs that stimulate the parts of the brain influenced by dopamine and lead the brain to believe that it receives the dopamine it needs. Possible side effects of this type of medication are nausea, hallucinations, sudden sleepiness and lightheadedness due to low blood pressure.

Anticholinergics

Anticholinergics is a medication against the tremor and may ease dystonia. It does not act directly on the dopaminergic system. Instead, it decreases the activity of acetylcholine, a neurotransmitter that regulates movement. Possible side effects are blurred vision, dry mouth, constipation and urinary retention.

MAO-B inhibitors

Selegiline and rasagiline block an enzyme in the brain that breaks down levodopa. These drugs have the lowest effect in suppressing the symptoms of PD but delay the need for other medications in the earliest stage of Parkinson's or boost the effects of other medications in later stages.

COMT inhibitors

COMT inhibitors such as entacapone and tolcapone are the newest class of medications and have no direct effect on Parkinson's disease symptoms, but prolong the effect of levodopa by blocking its metabolism.

3.3.2 Surgery

According to the Parkinson's Disease Foundation, surgeries were developed more than 50 years ago. The newest version of this surgery is the so called deep-brain stimulation.

Deep-brain stimulation (DBS)[14]
Deep-brain stimulation is a surgical technique in which one or more electrodes attached to leads are implanted in specific regions of the brain which are connected to an impulse generator. The way of implantation is shown in Figure (4).

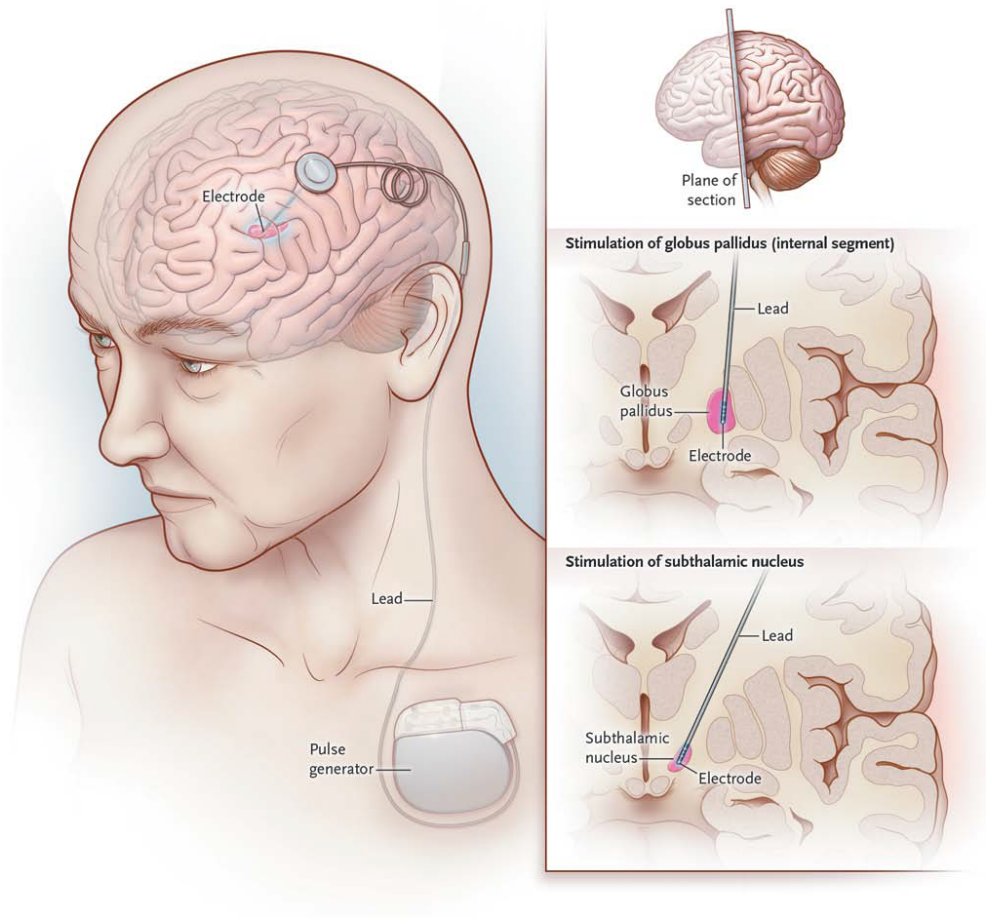

Figure 4: Electrode implantation for deep-brain stimulation[14]

The impulse generator delivers electrical stimuli to brain tissue to modulate or disrupt patterns of neural signaling and acts in targeted regions in the basal ganglia where much of the degenerative change in Parkinson's disease occurs. Deep-brain stimulation changes the firing rate and pattern of individual neurons in the basal ganglia, increases blood flow and stimu-

lates neurogenesis.
DBS has electrical, chemical and other neural-network influences on brain tissue. So far it is unclear how exactly these influences lead to changes in the symptoms of Parkinson's disease, which means that the benefits have been established more or less empirically.
During a trial conducted in Germany and Austria, 156 Parkinson's patients with motor symptoms were randomly assigned to undergo deep-brain stimulation. At 6 months, patients showed better mean scores on the PDQ-39 (31.8 vs. 40.2) and the UPDRS-III (28.3 vs. 46.0), which are scales measuring quality of life and severity of motor symptoms, respectively.
However, this surgery is only good for a certain target group. Candidates rated as good by the The New England Journal of Medicine include people showing adequate response to dopaminergic therapy, patients that have on–off fluctuations and people whose quality of life is impaired by dyskinesia. Good candidates are also PD patients having medication-resistant tremor but still possess reasonable cognitive functions.
Deep-brain stimulation can cause adverse effects, such as infection and intracranial hemorrhage associated with the placement of the leads. Neurologic side effects include cognitive impairment, memory deficits, difficulties with speech, disequilibrium, dysphagia and motor and sensory disturbances. Psychological adverse effects may be, among others, mania, depression, apathy, laughter and suicidal ideation.

4 Parkinson's from the mechanical engineering point of view

This work about Parkinson's disease focuses on the mechanical aspects of PD which can only encompass symptoms visible to the environment. Therefore, the goal is to focus on the tremor in the Parkinson's patients arms.
As the human's arm is a multiple degree of freedom system, there exists a vast number of axes around which tremor can occur. However, the focus of this work is on the rotational tremor around the axis formed by the forearm. In Figure (5), the axis formed by the forearm is labeled x and the rotational axis of interest around this axis is labeled with the capital letter A.

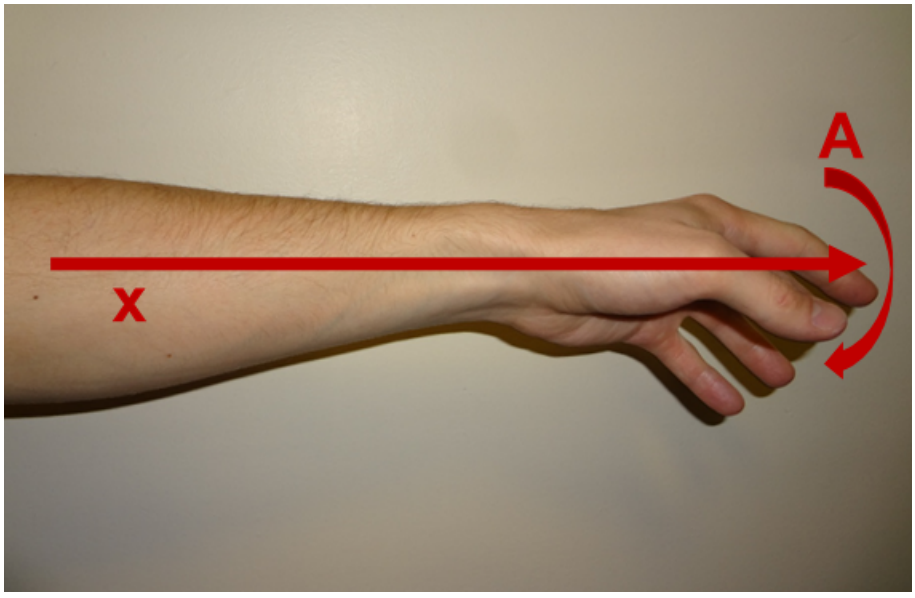

Figure 5: Tremor axes of interest

In contrast to the medical approach which focuses on the brain of the person, this mechanical approach views the tremor as vibrations. Therefore an equivalent mathematical model of the arm and its tremor about the axis A in Figure (5) must be created.
Based on this model, a wearable device can be created that is capable of counteracting the tremor about the A-rotational-axis.

5 Tremor analysis

5.1 Examining AM and FM characteristics of Tremor[2]

Tremor of Parkinson's patients is an approximately sinusoidal oscillation, whereby the amplitude and the frequency may fluctuate. In literature [2], the variation of the amplitude is referred to amplitude modulation (AM) and for the fluctuation of the frequency, the universal term frequency modulation (FM) is used. The waveform may be distorted, which arises in part because of mechanical factors and in part due to the specific intensity and sequence in which various muscles are activated. These characteristics are shown in Figure (6).

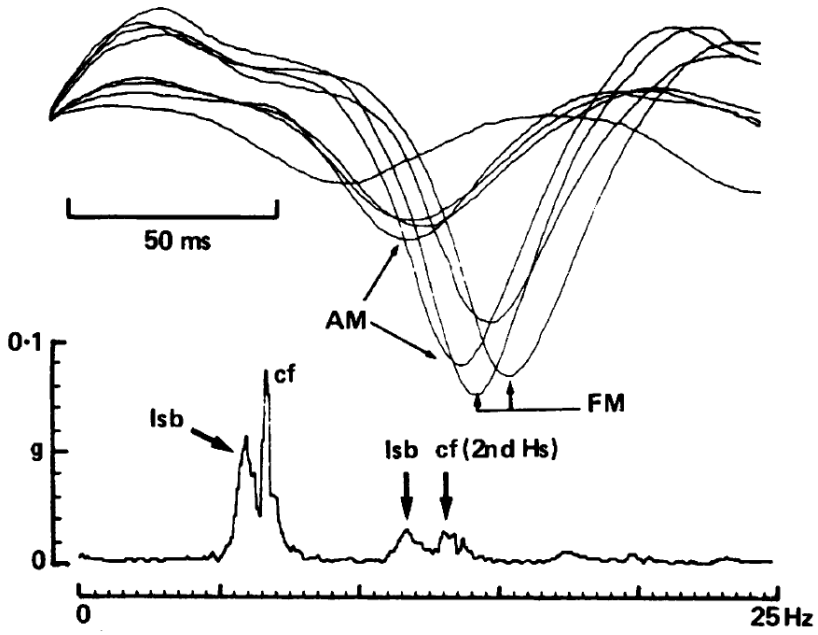

Figure 6: Accelerometric recordings and averaged spectrum of essential tremor[2]

Note that the individual cycles of the tremor are shown superimposed in Figure (6). The axis of acceleration is scaled in units of g, which is the earth's gravitational field. The abbreviations used are lower sideband (lsb), carrier frequency (cf) and harmonics (Hs). Interesting is that as amplitude increases, the period of the tremor cycle elongates, therefore for the tremor shown in Figure (6), the amplitude change is dependent on frequency change within certain constraints.

In the literature [2], different types of tremors showing AM as well as FM characteristics are displayed.
A tremor with small, slow fluctuations in amplitude and frequency can be found in Figure (7). In this case, the sidebands merge with the peak of the carrier frequency due to the slow change in amplitude over time, implying that the baseband signal is low frequency.

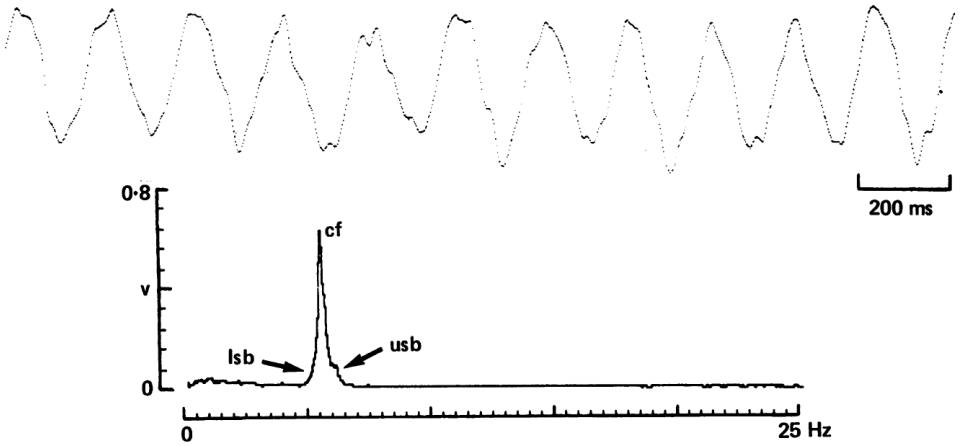

Figure 7: Tremor showing small, slow fluctuations in amplitude and frequency[2]

Figure (8) shows a tremor with harmonic distortion and moderately slow amplitude and frequency fluctuations, whereby the frequency variation is proportional to the amplitude variation. According to the literature [2], this type of tremor is typical of the rest tremor of Parkinson's disease.

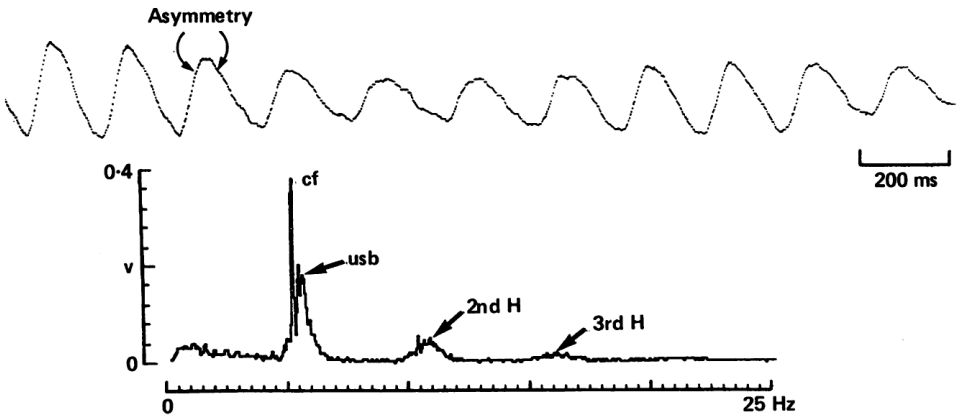

Figure 8: Tremor with harmonic distortion and moderately slow amplitude and frequency fluctuations[2]

5.2 Hand tremor in posture[3]

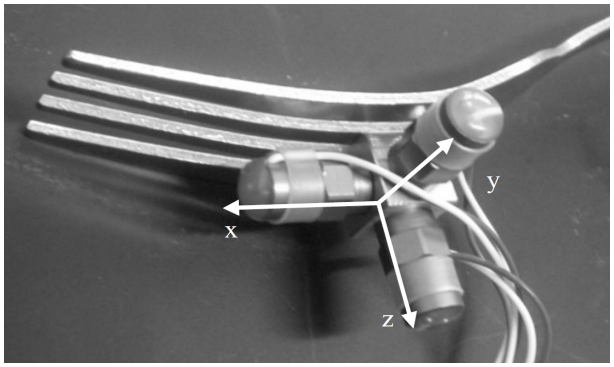

Figure 9: Triaxial accelerometer assembly[3]

An interesting case is the tremor occurring in the arm when holding a utensil such as a fork or pen. According to the cited literature, the tremor data shown in Figure (10) were collected while the Parkinson's patient was holding an eating utensil. This utensil was equipped with three accelerometers in orthogonal axes as shown in Figure (9). Slack in the accelerometer cables was provided to minimize effects on the tremor motion, and LabVIEW code was generated to read, record and process the motion data. An example of the data collected with this assembly can be found in Figure (10), whereby the data stem from the x direction accelerometer shown in Figure (9).

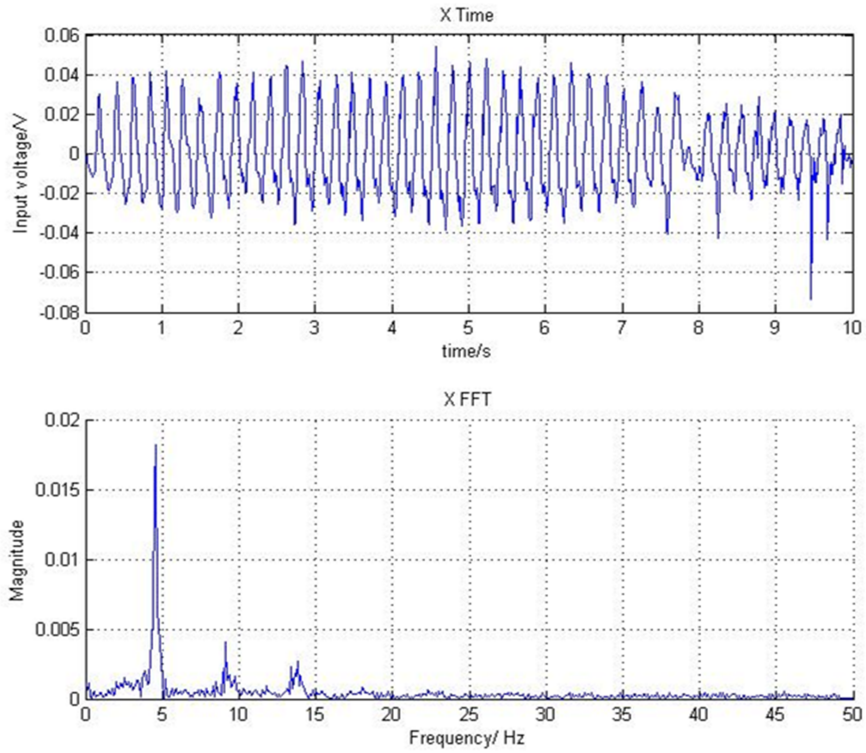

Figure 10: Time and frequency content for tremor while holding an utensil[3]

The spectrum in Figure (10) shows one primary spike at approximately 5Hz, even though declining harmonics exist at higher frequencies.

6 Modeling the arm using One Degree of Freedom

Before tackling the solution for the Parkinson's tremors, the first step is to create a mathematical model of the arm. The human arm is a complex system consisting of numerous bones, muscles and tendons and therefore, a sophisticated model would be necessary to describe the whole functionality of the human arm.
In this chapter, the very simplest model is used to describe this complicated system using a One Degree of Freedom (1DOF) Spring-Mass-Damper System shown in Figure (11). The constant m represents the mass of the arm, the c stands for its damping and k represents the stiffness of the human arm. The force $F(t)$ is the force modeling the cause of the tremor.
Note that the rotational movement of the arm is modeled as a translational movement, which seems to be a large difference. However, it turns out that modeling rotational movements as a translational system results in a very little change. The translational coordinate x would change into an angle φ, the mass would be a rotational moment of inertia and the damping and spring would be related to the angle φ, respectively.

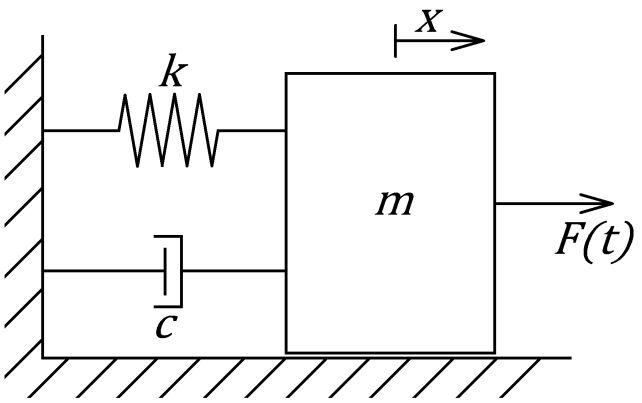

Figure 11: Modeling the arm using a One Degree of Freedom Spring-Mass-Damper System

6.1 One Degree of Freedom basic equations

Based on the model shown in Figure (11), a differential equation can be set up in order to describe the movement of m. Using Newton's law of motion

and neglecting friction between m and the surroundings leads to Equation (1).

$$m\ddot{x} + c\dot{x} + kx = F(t) \tag{1}$$

6.2 One Degree of Freedom Frequency Response Function (FRF)

In order to get information about the effect an input has on the output in steady state, the Frequency Response Function (FRF) is calculated. First the input and output is chosen, where $F(t)$ is the input and the mass' position $x(t)$ is used as output. Since the initial conditions for the steady state are zero, one way to get the FRF is by using the Laplace Transform with the initial condition

$$x(0) = 0.$$

Applying Laplace Transform with these conditions to Equation (1) leads to the result shown in Equation (2).

$$mX(s)s^2 + cX(s)s + kX(s) = F(s) \tag{2}$$

Equation (2) and the definition of the Transfer Function leads to the Transfer Function in the Laplace domain.

$$T(s) = \frac{X(s)}{F(s)} = \frac{1}{ms^2 + cs + k}$$

Using the connection between Laplace Transform and Fourier Transform

$$s = \sigma + j\omega \tag{3}$$

and setting σ to zero, i.e. $s = jw$, eventually leads to the Frequency Response Function stated in Equation (4).

$$T(\omega) = \frac{1}{k - m\omega^2 + jc\omega} \tag{4}$$

The magnitude of this complex Frequency Response Function is shown in Figure (12) and has one maximum at the system's resonant frequency.
As the Parkinson's tremor is excited around 5Hz, the goal is to choose parameters so that the magnitude of the FRF peaks at 5Hz. Therefore, a mathematical expression is needed in order to have a link between the

frequency where the peak occurs and the parameters m,c and k. Deriving the magnitude of $T(\omega)$ with respect to ω, setting the result equal to zero,

$$\frac{d}{d\omega}\{|T(\omega)|\} = 0$$

and solving this equation for ω, gives one real solution for ω_r at the peak of the FRF-curve, which is stated in a rearranged form in Equation (5).

$$k = \frac{c^2 + 2m^2\omega_r^2}{2m} \tag{5}$$

In the special case of a system without damping, where c equals to zero, Equation (5) simplifies to

$$\omega_r = \sqrt{\frac{k}{m}}.$$

Using the hertzian frequency in Equation (5) instead of the radian frequency leads to a mathematical expression linking the parameters of the system with the frequency f_r where the maximum of the magnitude of the FRF occurs.

$$k = \frac{c^2 + 8(m\pi f_r)^2}{2m} \tag{6}$$

For the application in regard to Parkinson's, Equation (6) is used to calculate a value for k where the maximum of the FRF-curve f_r is at 5Hz. For the first demonstration, the other parameters are chosen arbitrarily, $m = 1kg, c = 1\frac{Ns}{m}$. Evaluating Equation (6) with these parameters gives $k = 987.46\frac{N}{m}$.
A plot of the magnitude of the Frequency Response Function using these parameters is shown in Figure (12).

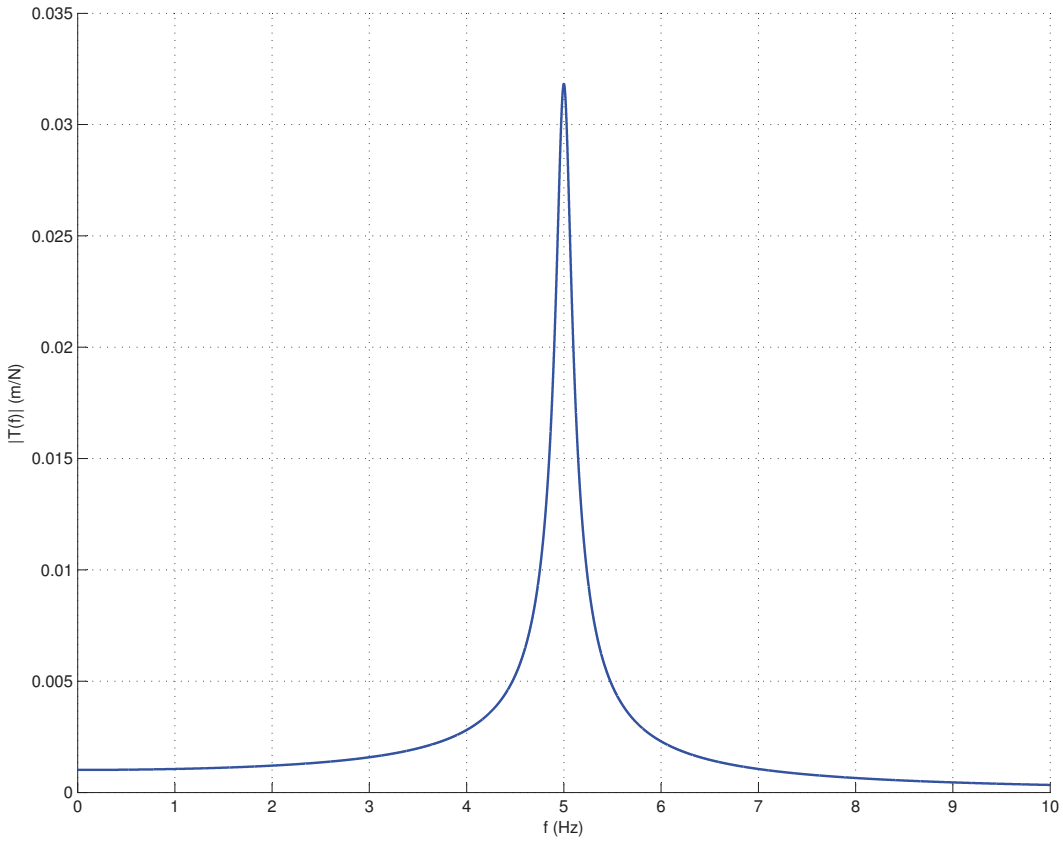

Figure 12: Magnitude of the FRF for the 1DOF Spring-Mass-Damper System

The magnitude of the FRF shown in Figure (12) is only plotted for low frequencies, as only low frequencies occur in Parkinson's patient's tremors and therefore are significant for this application. Moreover, the peak at 5Hz is the only maximum in the real plane, hence the magnitude of the FRF converging to zero for infinite frequency.

7 Modeling the system using Two Degrees of Freedom

This section is dedicated to an approach for reducing the tremor by changing the original One Degree of Freedom System in order to primarily damp the amplitudes of the mainly excited frequencies. The approach introduced in this section changes the original One Degree of Freedom System into a Two Degrees of Freedom System, depicted in Figure (13).

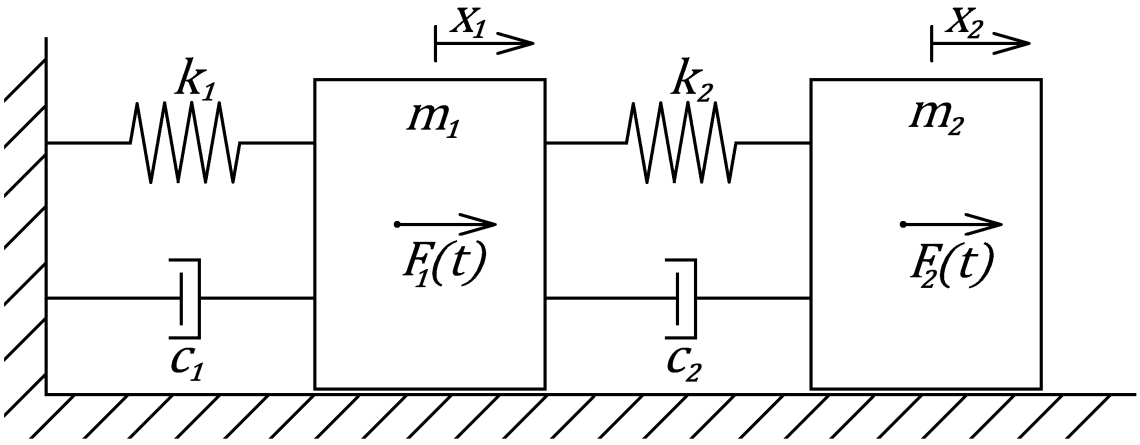

Figure 13: Modeling the system using a Two Degrees of Freedom Spring-Mass-Damper System

In this Figure, m_1,c_1 and k_1 are the same mass, damping and stiffness constants as used in Section (6) and therefore represent the human arm. Again, $F_1(t)$ is the force modeling the excitation of the tremor.
The second part of the system around m_2 is added in order to change the original system. Note that the parameters of the system shown in Figure (13) are simplified and analogous parameters of a system which will be more complex in implementation. m_2, c_2 and k_2 can be freely chosen by changing the mechanical implementation of the additional part. The challenge is to design this second part for parameters that change the original system so that the unwanted frequencies are significantly damped.
In the most general case, $F_2(t)$ represents a force acting on the added part of the system.
Note that this is a translational representation of an initially rotational system. As mentioned in Section (6), the transition to the rotational system is minor. In this Two Degrees of Freedom System, the translational

coordinates x_1 and x_2 would change into angular coordinates φ_1 and φ_2, the mass matrix would change into a rotational moment of inertia matrix and the damping and spring matrices would be related to the angles φ_1 and φ_2.

7.1 Two Degrees of Freedom basic equations

Just like in Section (6), friction is neglected and Newton's law of motion is applied to both bodies shown in Figure (13), having masses m_1 and m_2.

$$-k_1x_1 + (x_2 - x_1)k_2 - c_1\dot{x}_1 + (\dot{x}_2 - \dot{x}_1)c_2 + F_1(t) = m_1\ddot{x}_1 \tag{7}$$

$$-(x_2 - x_1)k_2 - (\dot{x}_2 - \dot{x}_1)c_2 + F_2(t) = m_2\ddot{x}_2 \tag{8}$$

Equation (7) and (8) result from applying Newton's law of motion to the two Degrees of Freedom System, where Equation (7) is the outcome from the first body and Equation (8) is the result from the second body. In order to write these two differential equations in a convenient way, they can be rearranged as follows.

$$\ddot{x}_1m_1 + (c_1 + c_2)\dot{x}_1 - c_2\dot{x}_2 + (k_1 + k_2)x_1 - k_2x_2 = F_1(t) \tag{9}$$

$$\ddot{x}_2m_2 - c_2\dot{x}_1 + c_2\dot{x}_2 - k_2x_1 + k_2x_2 = F_2(t) \tag{10}$$

This new sequence properly orders the variables and facilitates writing them in matrix format. An advantageous format using matrix notation is possible if one introduces three matrices named mass matrix $\boldsymbol{M}$, damping matrix $\boldsymbol{C}$ and stiffness matrix $\boldsymbol{K}$. Using these abbreviations, a Multiple Degree of Freedom System can be expressed as stated in Equation (11).

$$\boldsymbol{M}\ddot{\vec{x}} + \boldsymbol{C}\dot{\vec{x}} + \boldsymbol{K}\vec{x} = \vec{F} \tag{11}$$

For the system of differential equations written down in the Equations (9) and (10), the matrix notation has the form shown in Equation (12).

$$\begin{pmatrix} m_1 & 0 \\ 0 & m_2 \end{pmatrix} \begin{pmatrix} \ddot{x}_1 \\ \ddot{x}_2 \end{pmatrix} + \begin{pmatrix} c_1 + c_2 & -c_2 \\ -c_2 & c_2 \end{pmatrix} \begin{pmatrix} \dot{x}_1 \\ \dot{x}_2 \end{pmatrix} + \begin{pmatrix} k_1 + k_2 & -k_2 \\ -k_2 & k_2 \end{pmatrix} \begin{pmatrix} x_1 \\ x_2 \end{pmatrix} = \begin{pmatrix} F_1(t) \\ F_2(t) \end{pmatrix} \tag{12}$$

7.2 Two Degrees of Freedom Frequency Response Function (FRF)

The Frequency Response Function can be used to get information for the effect any input has on the output. First, the inputs and outputs of the FRF have to be defined. As one is interested in the magnitude of the vibrations of both the hand and the additional system due to external forces, the outputs are x_1 and x_2 and the inputs are the acting forces $F_1(t)$ and $F_2(t)$, respectively.
As there are two input and two output variables, there exist four Frequency Response Functions which can be defined as

$$T_{\frac{X_1}{F_1}}(\omega),\ T_{\frac{X_2}{F_1}}(\omega),\ T_{\frac{X_1}{F_2}}(\omega),\ T_{\frac{X_2}{F_2}}(\omega).$$

In order to get these FRFs, the differential equation system stated in the Equations (7) and (8) has to be solved using initial conditions which are zero. One way to accomplish this is to use the Laplace Transform to transform the equations, divide the output by the input and use the identity in Equation (3) implying that σ is zero.

7.2.1 Frequency Response Function of input F_1 to output X_1

It is important to annotate that the initial conditions are set to zero in order to get the Frequency Response Function, i.e.

$$x_1(0) = 0$$

$$x_2(0) = 0.$$

Using the Laplace Transform to transform Equations (7) and (8) from the time domain to the frequency domain yields Equations (13) and (14).

$$m_1X_1(s)s^2 = -k_1X_1(s)+k_2X_2(s)-k_2X_1(s)-c_1X_1(s)s+c_2X_2(s)s-c_2X_1(s)s+F_1(s) \tag{13}$$

$$m_2X_2(s)s^2 = -k_2X_2(s) + k_2X_1(s) - c_2X_2(s)s + c_2X_1(s)s + F_2(s) \tag{14}$$

Using Equation (14) allows expressing $X_2(s)$ in dependence of $X_1(s)$ as follows.

$$X_2(s) = \frac{k_2X_1(s) + c_2X_1(s)s + F_2(s)}{m_2s^2 + k_2 + c_2s}$$

This result can be plugged into Equation (13), and rearranging results in the desired Transfer Function. It is important to note that for the Transfer Function of input F_1 to output X_1, the input $F_2(t)$ is held zero, i.e. $F_2(t) = 0$.

$$T_{\frac{X_1}{F_1}}(s) = \frac{X_1(s)}{F_1(s)} = \frac{m_2 s^2 + k_2 + c_2 s}{(m_2 s^2 + k_2 + c_2 s) \cdot (m_1 s^2 + k_1 + k_2 + (c_1 + c_2)s) - (k_2 + c_2 s)^2}$$

Setting $s = j\omega$, eventually leads to the Frequency Response Function stated in Equation (15).

$$T_{\frac{X_1}{F_1}}(\omega) = \frac{k_2 - m_2\omega^2 + jc_2\omega}{(k_2 - m_2\omega^2 + jc_2 w) \cdot (k_1 + k_2 - m_1\omega^2 + j(c_1 + c_2)\omega) - (k_2 + jc_2\omega)^2} \tag{15}$$

Related literature can be found in [15] and covers a special case of a Two Degrees of Freedom Mass-Spring-Dashpot System using the term dynamic vibration absorber. In this special case, the damping c_1 is set to zero.

$$T_{\frac{X_1}{F_1}}(\omega) = \frac{k_2 - m_2\omega^2 + jc_2\omega}{((k_1 - m_1\omega^2)(k_2 - m_2\omega^2) - m_2 k_2\omega^2) + j\omega c_2(k_1 - m_1\omega^2 - m_2\omega^2)} \quad [15]$$

Plugging $c_1 = 0$ into Equation (15) and rearranging results in exactly the same expression.

The goal for this application is to chose parameters of the wearable device so that the minimum of the FRF occurs at 5Hz. Therefore, a mathematical expression is needed in order to have a link between the frequency where the minimum occurs and the parameters m_1, m_2, c_1, c_2, d_1 and d_2. Deriving the magnitude of $T_{\frac{X_1}{F_1}}(\omega)$ with respect to ω, setting the result equal to zero,

$$\frac{d}{d\omega}\{|T_{\frac{X_1}{F_1}}(\omega)|\} = 0$$

and solving this equation for ω fulfills this requirement. However, solving this equation is not trivial by hand, and therefore the symbolic computation program Mathematica was used to obtain numeric solutions for this equation. The computation yielded four solutions with two of them in the real plane. Choosing the solution associated with the minimum at 5Hz gives $k_2 = 986.458\frac{N}{m}$.

For the first demonstration, most of the system's parameters were chosen

arbitrarily, namely $m_1 = m_2 = 1kg$ and $c_1 = c_2 = 1\frac{Ns}{m}$. For $k_1 = 987.46\frac{N}{m}$, the same parameter as in Section (6.2) was used. $k_2 = 986.458\frac{N}{m}$ was calculated above in order to generate a minimum of the FRF's magnitude at 5Hz.
A plot of the magnitude of the Frequency Response Function using these parameters is shown in Figure (14).

As long as the second part of the system is dominating the Frequency Response Function and the damping keeps within limits, it is sufficient to use the approximation shown in Equation (16) to calculate the minimum of the FRF.

$$\omega_r = \sqrt{\frac{k_2}{m_2}} \tag{16}$$

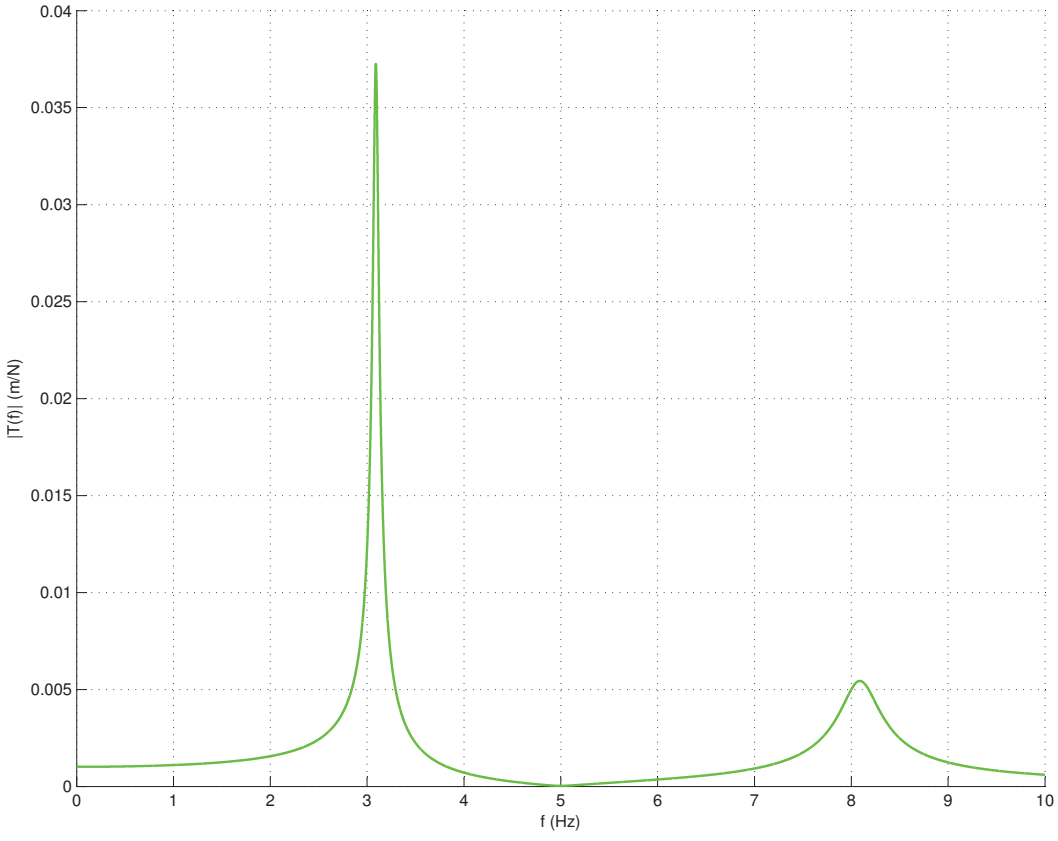

Figure 14: Magnitude of $T_{\frac{X_1}{F_1}}(\omega)$

The magnitude plot of the Frequency Response Function in Figure (14) describes the scaling factor for each frequency's amplitude. As desired, a drop occurs at the frequency of 5Hz, which can approach zero but only reaches exactly zero if there is no damping in the system.

For the purpose of getting a better understanding of the system, the plot in Figure (15) contains the magnitude of the FRF of both the original system from Figure (12) and the modified system from Figure (14).

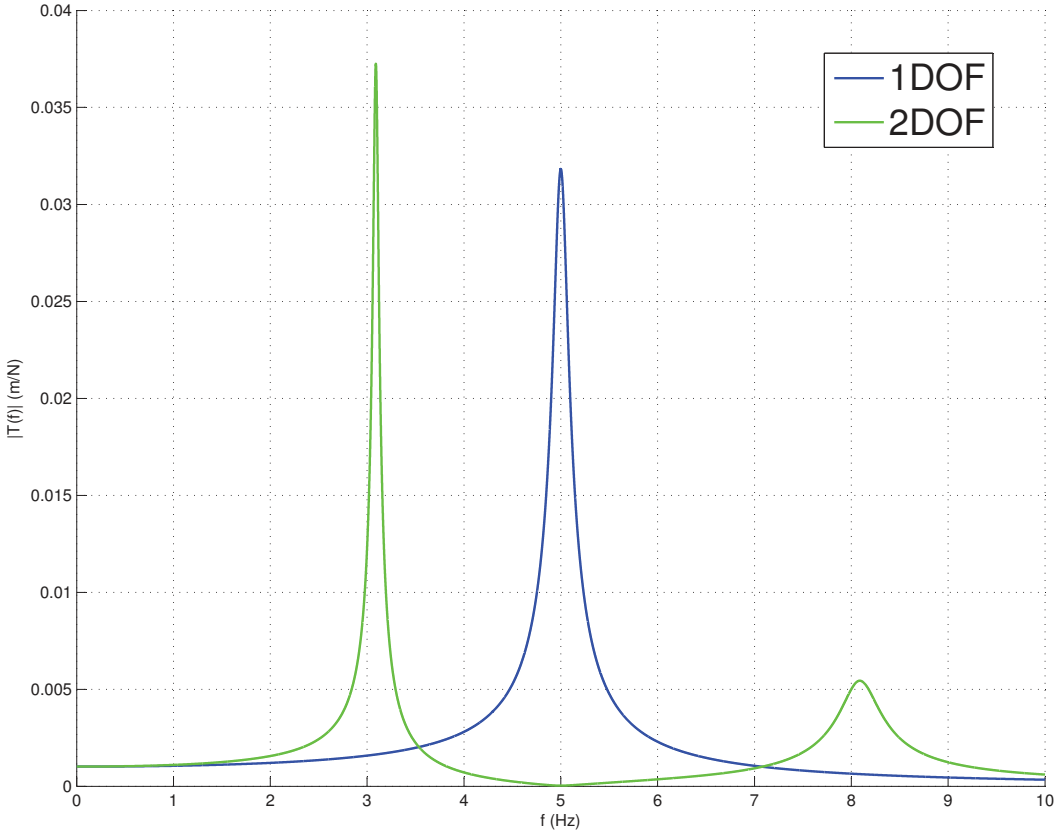

Figure 15: Magnitude of both the 1DOF - $T(\omega)$ and the 2DOF - $T_{\frac{X_1}{F_1}}(\omega)$ systems

7.2.2 Frequency Response Function of input F_1 to output X_2

In order to calculate the FRF of input F_1 to output X_2, the results of the Section (7.2.1) are reused. Using Equation (13) enables one to express $X_1(s)$ in terms of $X_2(s)$ as follows.

$$X_1(s) = \frac{k_2 X_2(s) + c_2 X_2(s)s + F_1(s)}{m_1 s^2 + k_1 + k_2 + c_1 s + c_2 s}$$

For the purpose of calculating the Frequency Response Function of input F_1 to output X_2, the input $F_1(t)$ is held zero, i.e. $F_1(t) = 0$. Plugging the expression of $X_1(s)$ back into Equation (14) and rearranging terms gives the corresponding Transfer Function.

$$T_{\frac{X_2}{F_1}}(s) = \frac{X_2(s)}{F_1(s)} = \frac{k_2 + c_2 s}{(m_2 s^2 + c_2 s + k_2)(m_1 s^2 + (c_1 + c_2)s + k_1 + k_2) - (k_2 + c_2 s)^2}$$

Setting $s = j\omega$, eventually leads to the Frequency Response Function stated in Equation (17).

$$T_{\frac{X_2}{F_1}}(\omega) = \frac{k_2 + jc_2\omega}{(k_2 - m_2\omega^2 + jc_2\omega)(k_1 + k_2 - m_1\omega^2 + j(c_1 + c_2)\omega) - (k_2 + jc_2\omega)^2} \tag{17}$$

Upon closer examination, the denominators of $T_{\frac{X_1}{F_1}}(\omega)$ and $T_{\frac{X_2}{F_1}}(\omega)$ are the same, hence it is possible to express $T_{\frac{X_2}{F_1}}(\omega)$ in terms of $T_{\frac{X_1}{F_1}}(\omega)$.

$$T_{\frac{X_2}{F_1}}(\omega) = T_{\frac{X_1}{F_1}}(\omega)\frac{k_2 + jc_2\omega}{k_2 - m_2\omega^2 + jc_2\omega} \tag{18}$$

In the related literature [15], a special case of this could be found where, again, $c_1 = 0$.

$$T_{\frac{X_2}{F_1}}(\omega) = \frac{T_{\frac{X_1}{F_1}}(\omega)(k_2 + j\omega c_2)}{k_2 - m_2\omega^2 + j\omega c_2} \text{ [15]}$$

This expression is the same result as found in Equation (18), as Equation (18) is not dependent on c_1.

Plotting the Frequency Response Function of Equation (17) with the same parameters as used in Section (7.2.1) leads to the following plot shown in Figure (16).

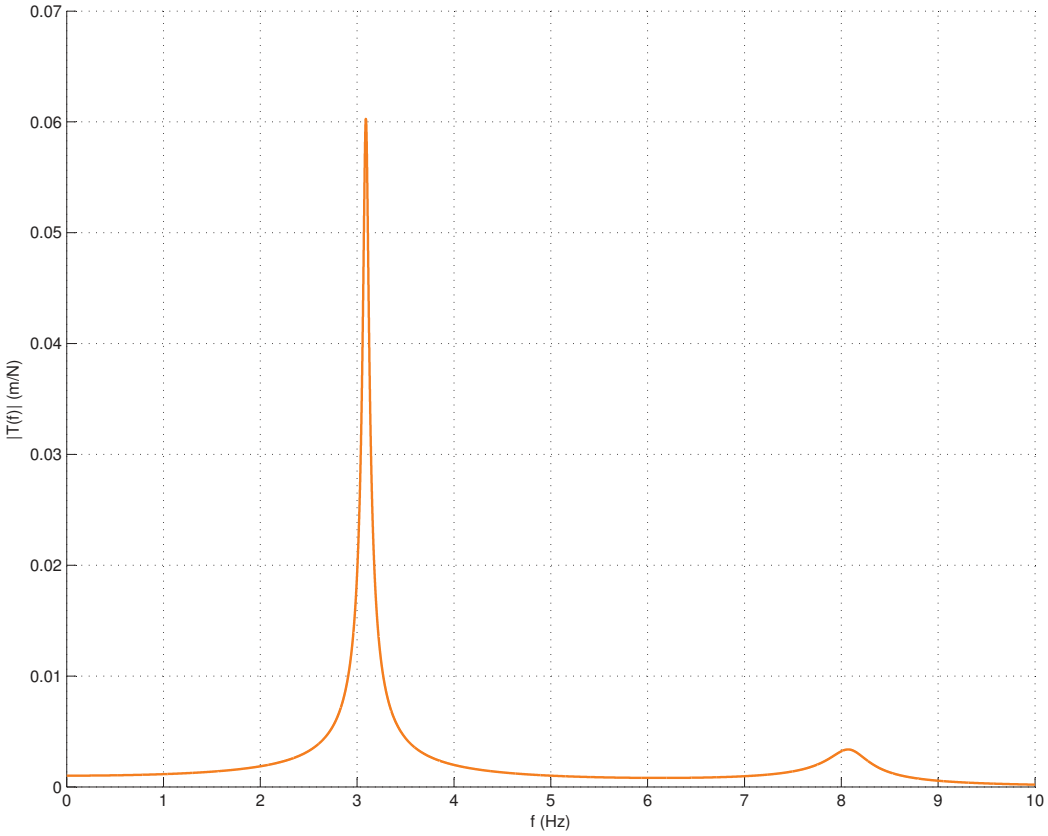

Figure 16: Magnitude of $T_{\frac{X_2}{F_1}}(\omega)$

This Frequency Response Function represents to what extent the output $x_2(t)$ changes due to an input at $F_1(t)$. It is obvious that the shape is similar to the shape of the FRF in Figure (14), only the drop is not as sharp. As the drop around 5Hz also exists in Figure (16), both the arm and the additional system have a very high damping of the amplitude around this frequency, which gives even better results than originally desired.

7.2.3 Frequency Response Function of input F_2 to output X_1

The Frequency Response Function of input F_2 to output X_1 can be found by using the same approach as used to find the other FRFs in Sections (7.2.1) and (7.2.2). Thus, using Laplace Transform and rearranging terms lead to the corresponding Transfer Function in the frequency domain

$$T_{\frac{X_1}{F_2}}(s) = \frac{X_1(s)}{F_1(s)} = \frac{1}{(m_2s^2 + c_2s + k_2)(m_1s^2 + (c_1 + c_2)s + k_1 + k_2) - (k_2 + c_2s)^2}$$

and to the desired Frequency Response Function

$$T_{\frac{X_1}{F_2}}(\omega) = \frac{1}{(k_2 - m_2\omega^2 + jc_2\omega)(k_1 + k_2 - m_1\omega^2 + j(c_1 + c_2)\omega) - (k_2 + jc_2\omega)^2}. \tag{19}$$

Plotting the Frequency Response Function of Equation (19), with the same parameters as used in Section (7.2.1), leads to the following plot shown in Figure (17).

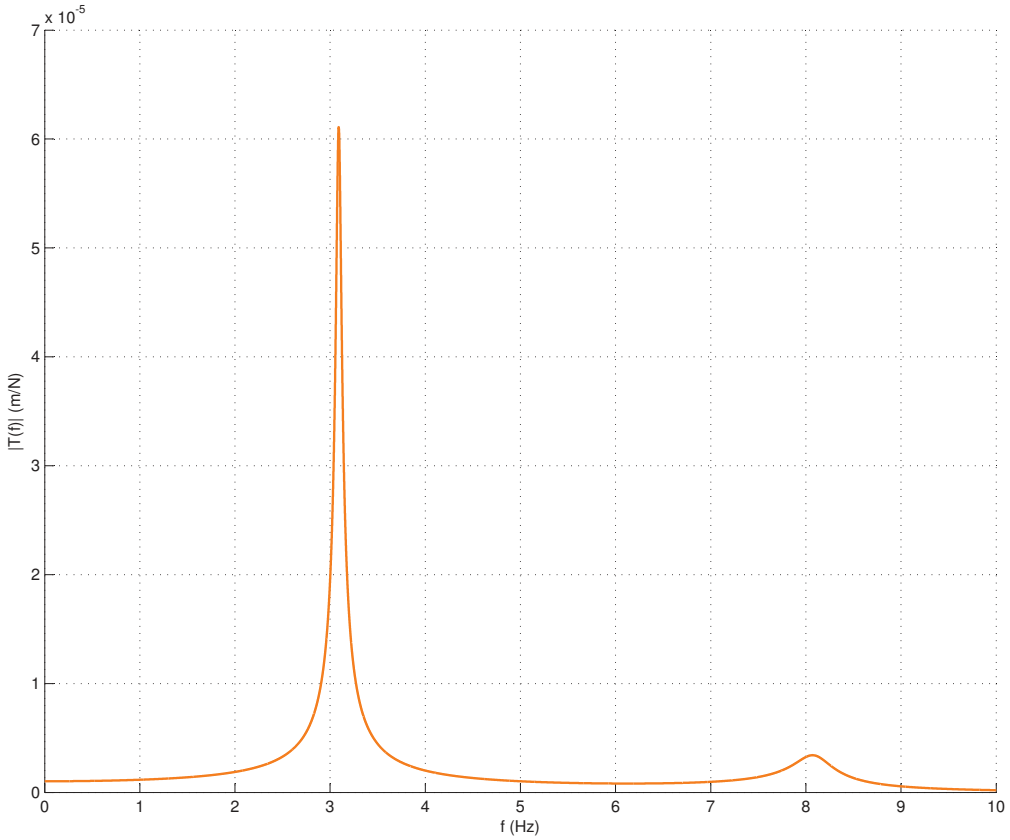

Figure 17: Magnitude of $T_{\frac{X_1}{F_2}}(\omega)$

This Frequency Response Function represents to what extent a force $F_2(t)$ changes the position $x_1(t)$ of the Parkinson's patient's arm. Of course, the case of an acting force on the additional system is not desired, but in the most general case it could occur and it is therefore necessary to examine it. The shape of this plot shown in Figure (17) is comparable to the FRF shown in Figure (14), only the heights of the peaks at the resonant frequencies are way lower.

7.2.4 Frequency Response Function of input F_2 to output X_2

The Frequency Response Function of input F_2 to output X_2 can be found by using the same approach as used to find the other FRFs. Thus, using Laplace Transform and rearranging terms leads to the corresponding Transfer Function in the frequency domain

$$T_{\frac{X_2}{F_2}}(s) = \frac{X_2(s)}{F_2(s)} = \frac{k_1 + k_2 + m_1 s^2 + (c_1 + c_2)s}{(m_2 s^2 + c_2 s + k_2)(m_1 s^2 + (c_1 + c_2)s + k_1 + k_2) - (k_2 + c_2 s)^2}$$

and to the desired Frequency Response Function

$$T_{\frac{X_2}{F_2}}(\omega) = \frac{k_1 + k_2 - m_1\omega^2 + j(c_1 + c_2)\omega}{(k_2 - m_2\omega^2 + jc_2\omega)(k_1 + k_2 - m_1\omega^2 + j(c_1 + c_2)\omega) - (k_2 + jc_2\omega)^2}. \tag{20}$$

Due to the fact that the denominators of $T_{\frac{X_1}{F_2}}(\omega)$ and $T_{\frac{X_2}{F_2}}(\omega)$ are the same, $T_{\frac{X_2}{F_2}}(\omega)$ can be expressed in terms of $T_{\frac{X_1}{F_2}}(\omega)$

$$T_{\frac{X_2}{F_2}}(\omega) = T_{\frac{X_1}{F_2}}(\omega)(k_1 + k_2 - m_1\omega^2 + j(c_1 + c_2)\omega).$$

Plotting the magnitude of the Frequency Response Function stated in Equation (20), with the same parameters as used in Section (7.2.1), leads to the plot shown in Figure (18).

This Frequency Response Function describes to what extent a force $F_2(t)$ acting on the additional system changes the position $x_2(t)$, which clearly is not the case of normal operation but is covered in order to examine the most general case. Again, the shape is comparable to the FRF shown in Figure (14), but the bump at around 8Hz is not as distinct. The primary difference is that the magnitude of the first bump is way higher than in Figure (14). Even though in this case the system is more excited, it is acceptable because this is not the normal way of operation.

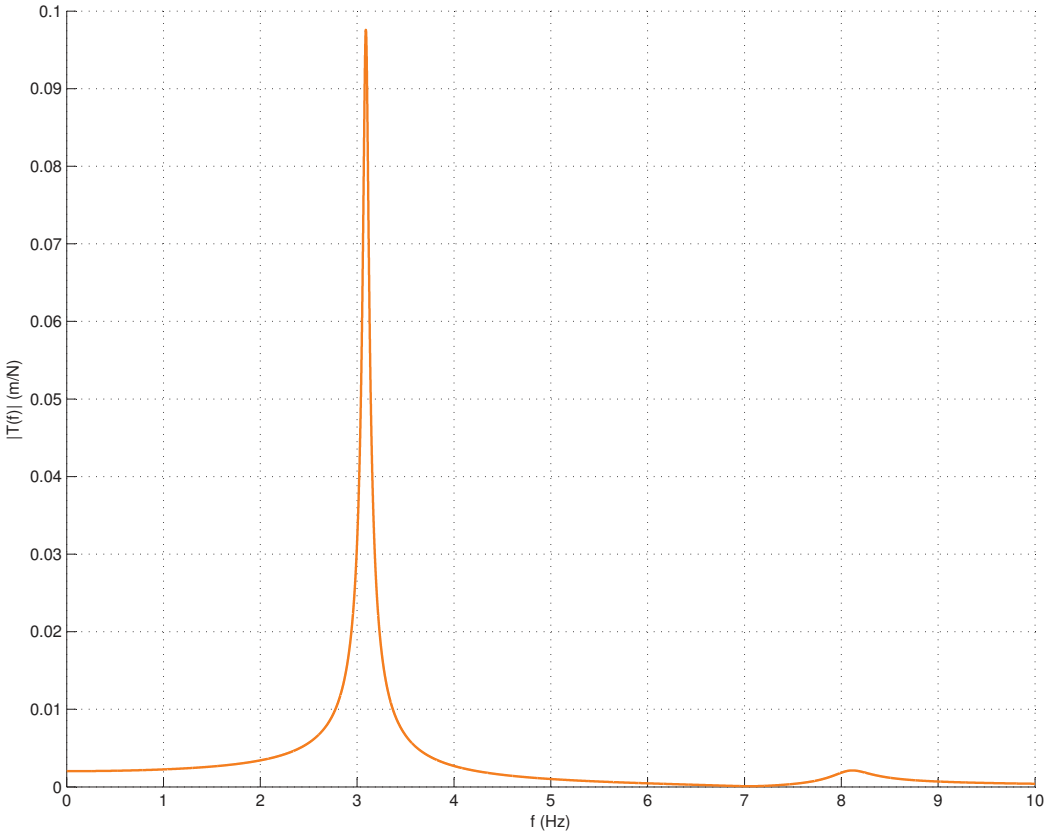

Figure 18: Magnitude of $T_{\frac{X_2}{F_2}}(\omega)$

8 Identifying parameters

8.1 Second-order mechanical impedance model[4]

This approach describes the movement of the arm using all elements of mechanical impedance, i.e. inertia, damping and stiffness. The second-order mechanical impedance model describes the dynamics of the arm and wrist by encompassing the movements shown in Figure (19).

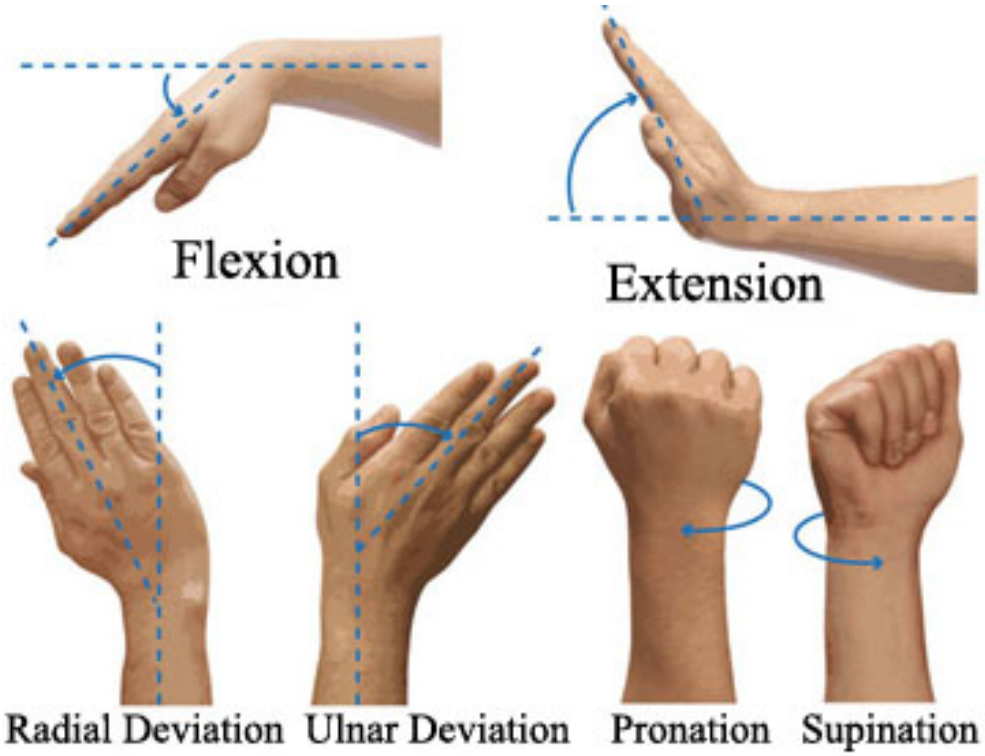

Figure 19: Types of rotations of the human's wrist and arm[16]

Abbreviations used in literature are FE for flexion–extension and RUD for radial–ulnar deviation, both describing the rotations of the wrist, and PS for pronation–supination describing the rotation of the forearm.

8.1.1 Mathematical model

The mathematical description of the dynamics models the wrist and forearm joints as a universal joint with the axes of all three DOF intersecting at the same point. Although the RUD axis is slightly distal to the FE axis, the distance is so small that it can be neglected. Including inertial, damping, stiffness and gravitational effects for each DOF, i.e. for PS, FE

and RUD rotations, leads to the following Equation (21).

$$\underbrace{\begin{pmatrix} M_\alpha \\ M_\beta \\ M_\gamma \end{pmatrix}}_{active\ torque} = \underbrace{\begin{pmatrix} A & B & C \\ B & D & E \\ C & E & F \end{pmatrix}\begin{pmatrix} \ddot{\alpha} \\ \ddot{\beta} \\ \ddot{\gamma} \end{pmatrix} + \begin{pmatrix} G \\ H \\ I \end{pmatrix}}_{inertial\ torque} + \underbrace{\begin{pmatrix} B_{\alpha\alpha} & B_{\alpha\beta} & B_{\alpha\gamma} \\ B_{\beta\alpha} & B_{\beta\beta} & B_{\beta\gamma} \\ B_{\gamma\alpha} & B_{\gamma\beta} & B_{\gamma\gamma} \end{pmatrix}\begin{pmatrix} \dot{\alpha} \\ \dot{\beta} \\ \dot{\gamma} \end{pmatrix}}_{damping\ torque}$$
$$+ \underbrace{\begin{pmatrix} K_{\alpha\alpha} & K_{\alpha\beta} & K_{\alpha\gamma} \\ K_{\alpha\beta} & K_{\beta\beta} & K_{\beta\gamma} \\ K_{\alpha\gamma} & K_{\beta\gamma} & K_{\gamma\gamma} \end{pmatrix}\begin{pmatrix} \alpha \\ \beta \\ \gamma \end{pmatrix}}_{stiffness\ torque} + \underbrace{glm_h \begin{pmatrix} \sin\alpha\sin\gamma - \cos\alpha\cos\gamma\sin\beta \\ -\cos\beta\cos\gamma\sin\alpha \\ \sin\alpha\sin\beta\sin\gamma - \cos\alpha\cos\gamma \end{pmatrix}}_{gravitational\ torque} \tag{21}$$

In this equation PS, FE and RUD are represented as Euler angles α, β and γ, respectively (in that order), according to ISB recommendations for global forearm and wrist rotations.[17]
The matrix with the letters A to F is the inertia matrix, while G to I are the centripetal and coriolis terms. The expanded terms of these abbreviations are shown in Figure (20).

A	$I_{Hx}\sin^2\beta + I_{Hy}\cos^2\beta\cos^2\gamma + I_{Hz}\sin^2\gamma\cos^2\beta + I_{Ay}$
B	$\cos\gamma\ \cos\beta\ \sin\gamma(I_{Hy} - I_{Hz})$
C	$I_{Hx}\ \sin\beta$
D	$I_{Hy}\sin^2\gamma + I_{Hz}\cos^2\gamma$
E	0
F	I_{Hx}
G	$I_{Hx}[\dot{\beta}\ \cos\beta(\dot{\gamma} + 2\dot{\alpha}\ \sin\beta)]$ $+ I_{Hy}[\ \cos\beta\ \cos\gamma(\dot{\beta}\dot{\gamma}\ \cos\gamma - \dot{\alpha}\dot{\beta}\ \sin\beta\ \cos\gamma - \dot{\alpha}\dot{\gamma}\ \cos\beta\ \sin\gamma)$ $-(\dot{\beta}\ \sin\gamma + \dot{\alpha}\ \cos\beta\ \cos\gamma)(\dot{\beta}\ \sin\beta\ \cos\gamma + \dot{\gamma}\ \cos\beta\ \sin\gamma)]$ $+ I_{Hz}[\ \cos\beta\ \sin\gamma(\dot{\beta}\dot{\gamma}\ \sin\gamma + \dot{\alpha}\dot{\gamma}\ \cos\beta\ \cos\gamma - \dot{\alpha}\dot{\beta}\ \sin\beta\ \sin\gamma)$ $+(\dot{\beta}\ \cos\gamma - \dot{\alpha}\ \cos\beta\ \sin\gamma)(\dot{\beta}\ \sin\beta\ \sin\gamma - \dot{\gamma}\ \cos\beta\ \cos\gamma)]$
H	$-I_{Hx}\dot{\alpha}\ \cos\beta(\dot{\gamma} + \dot{\alpha}\ \sin\beta)$ $+ I_{Hy}[\dot{\alpha}\ \sin\beta\ \cos\gamma(\dot{\beta}\ \sin\gamma + \dot{\alpha}\ \cos\beta\ \cos\gamma)$ $+\dot{\gamma}\ \cos\gamma(2\dot{\beta}\ \sin\gamma + \dot{\alpha}\ \cos\beta\ \cos\gamma)$ $-\dot{\alpha}\ \sin\gamma(\dot{\beta}\ \sin\beta\ \cos\gamma + \dot{\gamma}\ \cos\beta\ \sin\gamma)]$ $+ I_{Hz}[\dot{\alpha}\ \sin\beta\ \sin\gamma(\dot{\alpha}\ \cos\beta\ \sin\gamma - \dot{\beta}\ \cos\gamma)$ $+\dot{\alpha}\ \cos\gamma(\dot{\beta}\ \sin\beta\ \sin\gamma - \dot{\gamma}\ \cos\beta\ \cos\gamma)$ $-\dot{\gamma}\ \sin\gamma(2\dot{\beta}\ \cos\gamma - \dot{\alpha}\ \cos\beta\ \sin\gamma)]$
I	$I_{Hx}(\dot{\alpha}\dot{\beta}\ \cos\beta) + (I_{Hy} - I_{Hz})(\dot{\beta}\ \sin\gamma + \dot{\alpha}\ \cos\beta\ \cos\gamma)(\dot{\alpha}\ \cos\beta\ \sin\gamma - \dot{\beta}\ \cos\gamma)$

Figure 20: Definition of terms of Equation (21)[4]

The left-hand side of Equation (21) represents active torques which could

be due to muscle contraction. The first matrix on the right-hand side contains the occurring inertial torque. The second matrix contains damping coefficients (e.g. $B_{\alpha\alpha}$) and therefore represents the damping torque. Similarly, the third matrix on the right-hand side of Equation (21) contains stiffness coefficients (e.g. $K_{\alpha\alpha}$) and therefore models the stiffness torque of the wrist and arm.
It has been shown that the stiffness coefficients of the wrist and forearm are symmetric and therefore the off-diagonal stiffness terms are set equal to each other.[18]
The last matrix represents the gravitational torque. The parameters g, l and m are the gravitational acceleration, distance from the wrist joint to the center mass of the hand and the mass of the hand, respectively.

8.1.2 Reducing the mathematical model to One Degree of Freedom

For the way to model the human arm that was used in Section (6), a 1DOF mathematical model allowing only rotations around the axis A shown in Figure (5) is necessary. This goal can be reached using the 3DOF model mentioned in Equation (21) and locking all other rotations by setting these degrees of freedom to zero, i.e. $\beta = \gamma = 0$. Plugging this into Equation (21) yields a sole, decoupled differential equation for the degree of freedom of interest α. This differential equation is stated in Equation (22).

$$M_\alpha(t) = I_{Ay}\ddot{\alpha} + B_{\alpha\alpha}\dot{\alpha} + K_{\alpha\alpha}\alpha \tag{22}$$

In this equation, M_α represents active torques around axis A from Figure (5), which are due to muscle and cause pronation-supination movement (PS).
The parameter I_{Ay} is the inertia of the forearm about its long axis through the center of mass (A in Figure (5)). The parameters $B_{\alpha\alpha}$ and $K_{\alpha\alpha}$ are the damping and stiffness constants (in that order) occurring about the same axis.

8.1.3 Experimental Setup

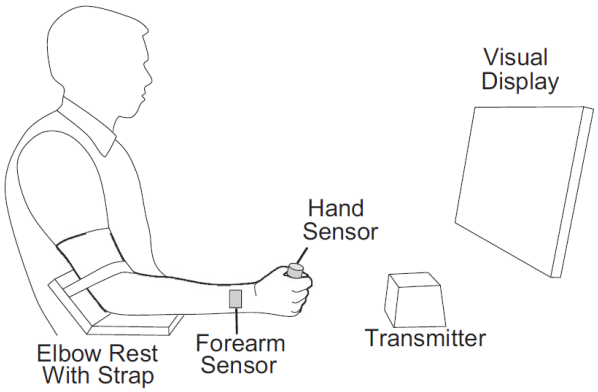

Figure 21: Experimental Setup[4]

According to the cited literature, the experimental setup shown in Figure (21) was used. Subjects were seated with about 0° shoulder abduction, approximately 30° of shoulder flexion and 60° elbow flexion. About 14cm of the forearm rested on a support, while the distal forearm, wrist and hand remained unsupported in order to allow unobstructed use of PS, FE and RUD. Electromagnetic motion-tracking sensors were attached to the forearm 5cm proximal to the wrist joint center and atop a handle held by the subject.
According to the used literature, joint angles were derived from the sensors' orientation data by inverse kinematics using α, β and γ for PS, PE and RUD, respectively. Sensor data were low-pass filtered with a fourth order Butterworth filter with a cut-off frequency of 20Hz and differentiated once to obtain velocity. Differentiating a second time after using the same filter again yields acceleration, to which the filter was applied one final time.
Inertia was obtained using published anthropometric regression equations [19], which estimate the inertia of the hand and forearm and the center of mass of the hand from measurements of segment lengths from each subject. This estimation is based on the assumption that the body-fixed inertia matrices of the hand and forearm are symmetric, i.e. negligible products of inertia.
The stiffness of coupled wrist and forearm rotations was measured for each subject in the lab using a rehabilitation robot moving each subject's wrist and forearm in combinations of PS, FE and PS in a quasi static manner while measuring the displacement and the torque required to perform the displacement.[18] The 3-DOF stiffness matrix was then estimated from the torque and displacement data using multi-variable linear regression.

Parameter	Male	Female
m [kg]	0.439	0.346
l [m]	0.0665	0.0586
I_{Hx} [kg m^2]	0.00317	0.00180
I_{Hy} [kgm^2]	0.000501	0.000241
I_{Hz} [kg m^2]	0.00276	0.00164
I_{Ay} [kgm^2]	0.00137	0.000505
$K_{\alpha\alpha}$ [Nm/rad]	0.756	0.827
$K_{\alpha\beta} = K_{\beta\alpha}$ [Nm/rad]	0.0175	0.0809
$K_{\alpha\gamma} = K_{\gamma\alpha}$ [Nm/rad]	0.291	0.148
$K_{\beta\beta}$ [Nm/rad]	0.992	0.713
$K_{\beta\gamma} = K_{\gamma\beta}$ [Nm/rad]	−0.0991	−0.0780
$K_{\gamma\gamma}$ [Nm/rad]	2.92	2.24
$B_{\alpha\alpha}$ [Nm s/rad]	0.0236	0.0362
$B_{\alpha\beta} = B_{\beta\alpha}$ [Nm s/rad]	0.000791	0.00376
$B_{\alpha\gamma} = B_{\gamma\alpha}$ [Nm s/rad]	0.00831	0.00643
$B_{\beta\beta}$ [Nm s/rad]	0.0300	0.0300
$B_{\beta\gamma} = B_{\gamma\beta}$ [Nm s/rad]	−0.00316	−0.00351
$B_{\gamma\gamma}$ [Nm s/rad]	0.0882	0.0959

Figure 22: Mean male and female parameters[4]

According to the cited literature, the passive damping occurring with coupled wrist and forearm rotations is unknown. However, measurements for flexion-extension yield to be 0.02-0.03 Nm s/rad. Studies have shown that the stiffness and damping ellipses associated with shoulder and elbow movements are roughly proportional.[20][21][22] Hence, the damping of the wrist and the forearm was assumed to be proportional to wrist and forearm stiffness. The constant of proportionality was chosen so that the damping in FE would be 0.03 Nm s/rad.
The obtained parameters refer to the mathematical model introduced in Equation (21) and are shown in Figure (22).

8.1.4 Parameters for the One Degree of Freedom model

The parameters for the One Degree of Freedom mathematical model shown in Equation (22) come from Figure (22). Male as well as female patients are expected, and therefore an arithmetic mean value of the parameters of both genders is used. The numerical values of these constants are shown

in Table (1).

Parameter	Male	Female	Arithmetic mean	Unit
I_{Ay}	0.00137	0.000505	0.0009375	$kg \cdot m^2$
$B_{\alpha\alpha}$	0.0236	0.0362	0.0299	$Nm \cdot s/rad$
$K_{\alpha\alpha}$	0.756	0.827	0.7915	Nm/rad

Table 1: Model parameters for One Degree of Freedom

9 Testing

9.1 Requirements

9.1.1 Reproducibility

Reproducibility refers to the variation in measurements made on a subject under changing conditions where the changing conditions may be due to different measurement methods or instruments being used, or measurements made by different observers or raters.[23]
In the case of the Parkinson's Assistive Technology, the human test objects, i.e. patients suffering from PD, are an available testing environment. The problem is that every person is different, and even if one patient is used for testing, his or her tremors could change depending on the condition on a particular day. This change in the patient's condition could result in a change in the amplitude of the shaking as well as in varying frequencies of the tremor.
Under these circumstances, it is necessary to create appropriate testing equipment that simulates the patient's tremors.

9.1.2 Adaptability

Adaptability in this context refers to the adaptability of the system's parameters. In order to perform tests for different types of patients, the parameters m_1, c_1 and k_1 have to be alterable. In this way, different mass, stiffness and damping of patients can be simulated.
Moreover, the frequency of the tremor also has to be adaptable to imitate a frequency range of different patients.

9.1.3 Availability

During the development, it is important to permanently have access to a testing environment. Along these lines, it is impracticable to use human patients and therefore a device simulating the tremors is essential.

9.2 Simulating the human's arm

9.2.1 Basic concept

A basic design that is capable of simulating a patient's tremor is shown in Figure (23). The mechanical shaker produces a translational movement which is converted into a rotational movement by using a linkage mounted on a pivot.

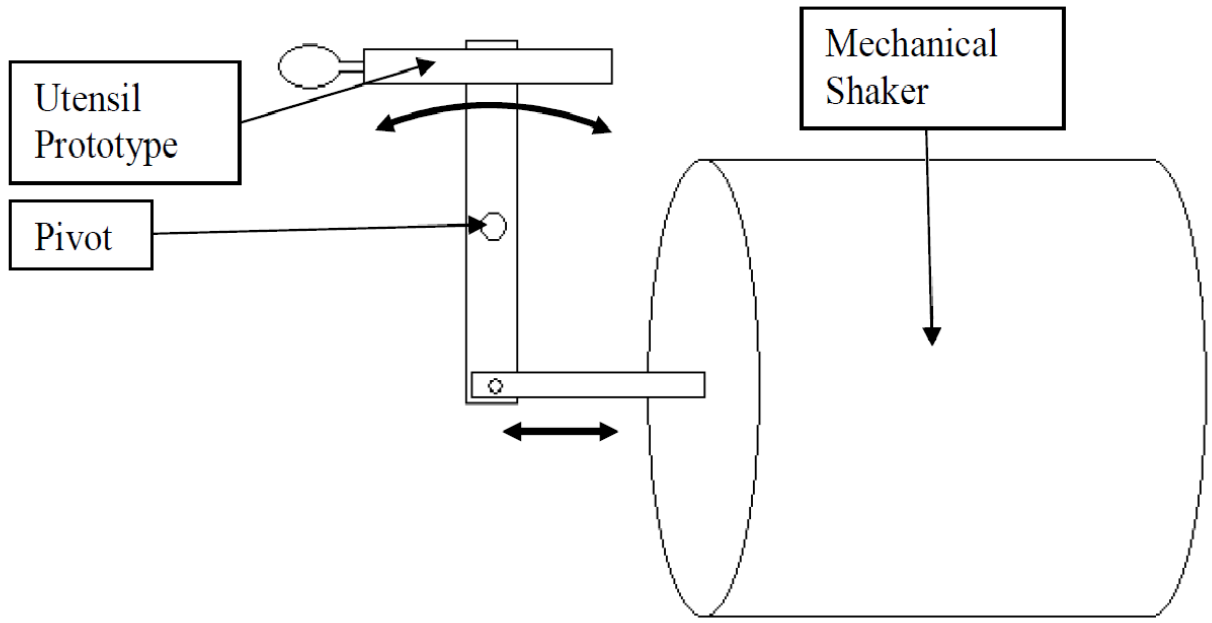

Figure 23: Initial concept for the testing apparatus[24]

The setup in Figure (23) imitates a tremor shown by the arrows next to the utensil prototype. Mounting the utensil prototype rotated by 90 degrees above the pivot and perpendicular to the linkage makes it possible to simulate a second type of tremor.

The mechanical shaker can provide oscillations with different amplitudes and frequencies. This accomplishes the adaptability requirements of the source of tremor mentioned in Section (9.1.2).

The mass of the linking can be thought as the mass of the hand m_1 from Figure (13). This initial concept, however, still lacks the implementation of the damping c_1 and the stiffness k_1 of the hand.

9.2.2 Testing apparatus

The testing apparatus depicted in Figure (24) is driven by a mechanical shaker which can provide different amplitudes and frequencies. This property makes it possible to imitate different types of tremors and vary them in intensity as well as frequency and ensures the design criteria of adaptability mentioned in Section (9.1.2).

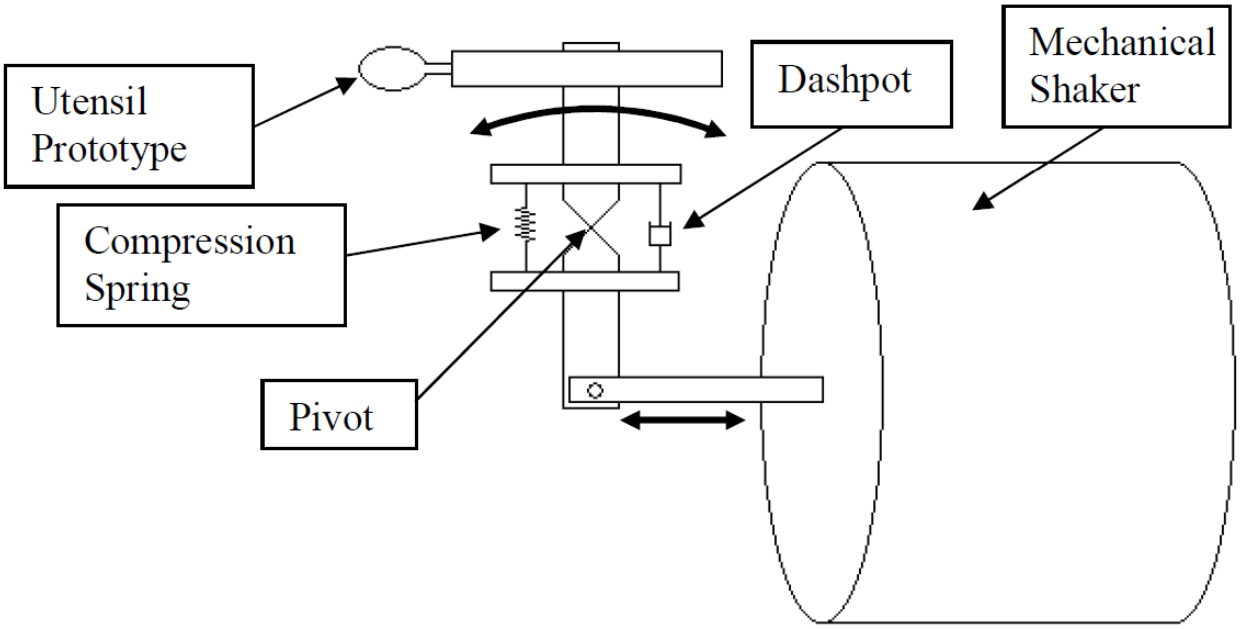

Figure 24: Testing apparatus modeling the human's arm[24]

Assuming the shaker is an ideal part, the reproducibility only depends on the accuracy with which the rest of the system is put together. For prototype testing, it is sufficient to manufacture the necessary parts by hand to reach a satisfying reproducibility.

In the implemented testing apparatus, an exciter of the type Modal 50A was used for the shaker. According to the technical data sheet, a stroke of 1" and a peak force of 25 pounds are provided at the exciter's output. For the testing of the Parkinson's Assistive Technology, low frequencies are crucial. Therefore, the lower limit of the shaker's output frequency is of paramount importance. According to the specification, this lowest reachable frequency is 1Hz and thus is significantly below the estimated Parkinson's tremor frequency.[25]

The testing apparatus shown in Figure (24) contains all parameters shown in Figure (13) for modeling the human arm. The mass of the linkage in addition to the mass of the other parts, e.g. the spring and the dashpot, represent the mass m_1 of the hand. The dashpot provides the damping c_1, and the compression spring constitutes the stiffness of the human arm.
Moreover, the force of the shaker in combination with the length of the linkage is analogous to the force $F_1(t)$ from Figure (13), hence modeling the cause of the Parkinson's disease tremor.
It is important to note that the translational system shown in Figure (13) is now constructed as rotational. As mentioned earlier, the equations derived in Section (6) can easily be adapted by changing the translational coordinate x into an angle φ and the changing the mass into a rotational moment of inertia.

The distance between the spring and the pivot and between the dashpot and the pivot, respectively, has influence on these parameters c_1 and k_1. To show this, a more detailed sketch of the area around the pivot is helpful, which is shown in Figure (25).

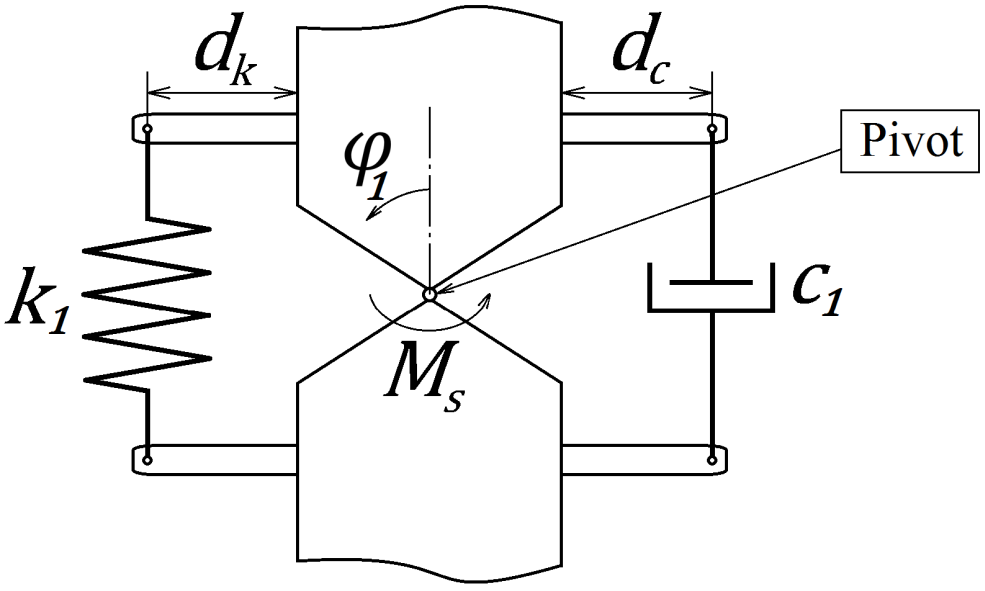

Figure 25: Detailed drawing of the pivot area of the testing apparatus

To examine the effect of the distances d_k and d_c, it is expedient to set up the differential equation of the system shown in Figure (25). Applying the

analogue of Newton's law for rotational motion for this system leads to

$$\ddot{\varphi}_1 J_1 = M_{k_1} + M_{c_1} + M_s(t),$$

where friction in the pivot is neglected. J_1 represents the rotational moment of inertia of the whole setup, M_{c_1} the torque produced by the dashpot c_1 and M_{k_1} the torque produced by the spring k_1. The torques produced by the spring and the dashpot can be described as follows

$$M_{k_1} = -k_1 \cdot \Delta l \cdot d_k$$

$$M_{c_1} = -c_1 \cdot v \cdot d_c$$

with Δl being the elongation of k_1 and v being the velocity of c_1's piston. For small deflections of the system, Δl is about equal to φ_1 and v is approximately $\dot{\varphi}_1$. Using these identities and plugging them into the previous equations leads to the differential equation stated in Equation (23), approximately describing the system shown in Figure (25).

$$J_1\ddot{\varphi}_1 + c_1 d_c \dot{\varphi}_1 + k_1 d_k \varphi_1 = M_s(t) \tag{23}$$

For determining what effect the distances d_c and d_k have on the system, it is not necessary to solve this second order differential equation. d_c is a multiplicative constant in front of c_1 and therefore just alters the value of c_1. The variable d_k is a multiplicative constant in front of k_1 and thus changes the value of k_1.

Taking advantage of these circumstances by making d_c and d_k adjustable allows changing the parameters and therefore ensures the design criteria adaptability mentioned in Section (9.1.2).

Figure (26) and (27) show a photo of the assembled testing apparatus. The label (a) in Figure (26), which is a front view of the testing apparatus, provides a location for extra mass in order to adjust the moment of inertia of the virtual hand, and again ensures the design criteria adaptability. The basic rotational moment of inertia of the virtual hand is created by the mass of the bar labeled (c). The rotation is centered around the pivot (b), which is implemented using thrust bearings in order to create a virtually frictionless joint. These bearings are mounted on the base (f) which

provides a foundation that prevents the testing apparatus from interacting with the environment and coupling with external vibrations.

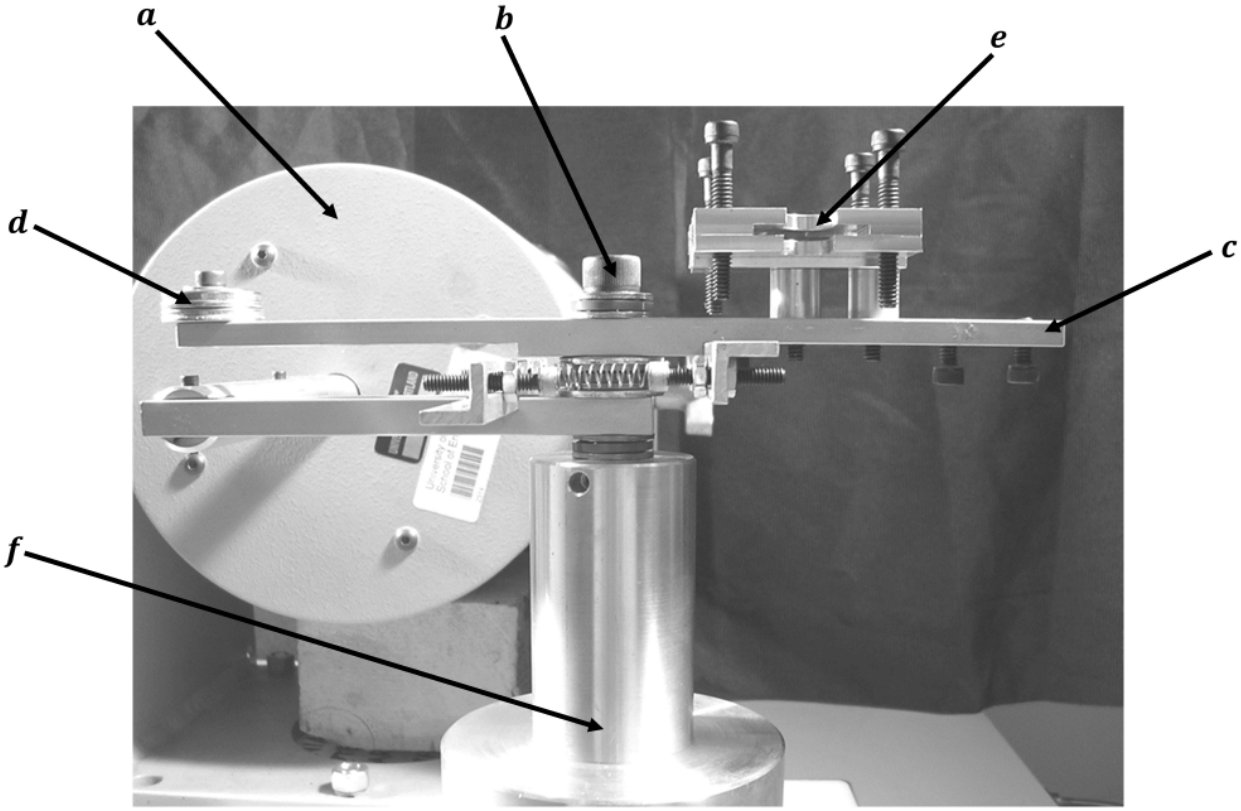

Figure 26: Front view of the testing apparatus[24]

The label (a) in Figure (26) is the Mechanical Shaker mentioned in Figure (24) of the type Modal 50A.

Figure (27) depicts a top view of the testing apparatus. In this figure, the damping c_1 and the stiffness k_1 of the Two Degrees of Freedom model shown in Figure (13) is built using an oil dashpot (c) and a compression spring (d). These elements were mounted in a certain distance from the pivot (b). This distance can be changed by loosening the nuts, moving the parts along the crossbar and tightening the nuts again. Altering these distances results in a change of the system's damping and stiffness as explained earlier in this section.
From the top view in Figure (27), it is apparent that the Mechanical Shaker output (a) creates a moment about the pivot (b). The output force of the exciter acting on (a) is modeled as $F_1(t)$ in Figure (13) and can be thought of as coming to the hand via muscles and tendons causing the tremor of the Parkinson's patient.

The interface for mounting the Parkinson's Assistive Device on the testing apparatus is provided by (e).

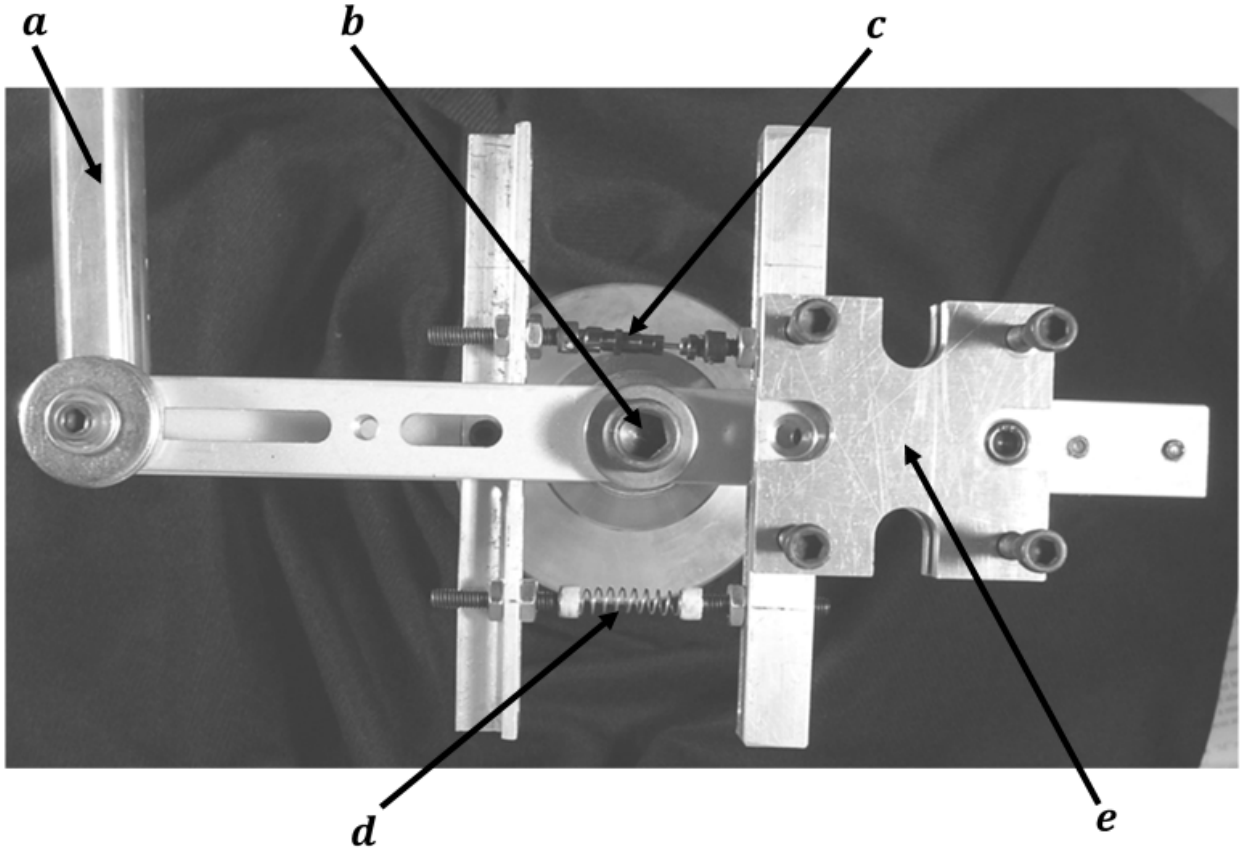

Figure 27: Top view of the testing apparatus[24]

9.2.3 Measurement hardware

The measurement hardware whose block diagram is shown in Figure (28) is designed to create a Frequency Response Function of the prototype under test. Therefore, any form of digital to analog conversion is necessary in order to create the input signal. For this purpose, hardware from National Instruments is used and controlled by a LabVIEW program. The module NI 9263 is used as a digital to analog converter, having four channels with 100kS/s, ±10V output range and a 16-bit resolution.
As shown in the block diagram, the digital analog converted excitation signal is processed through a low pass filter and amplified. The amplifier used is a MB Dynamics SS250VCF and is geared to the shaker from the same company, which is of the type Modal 50A as mentioned in Section (9.2.2).

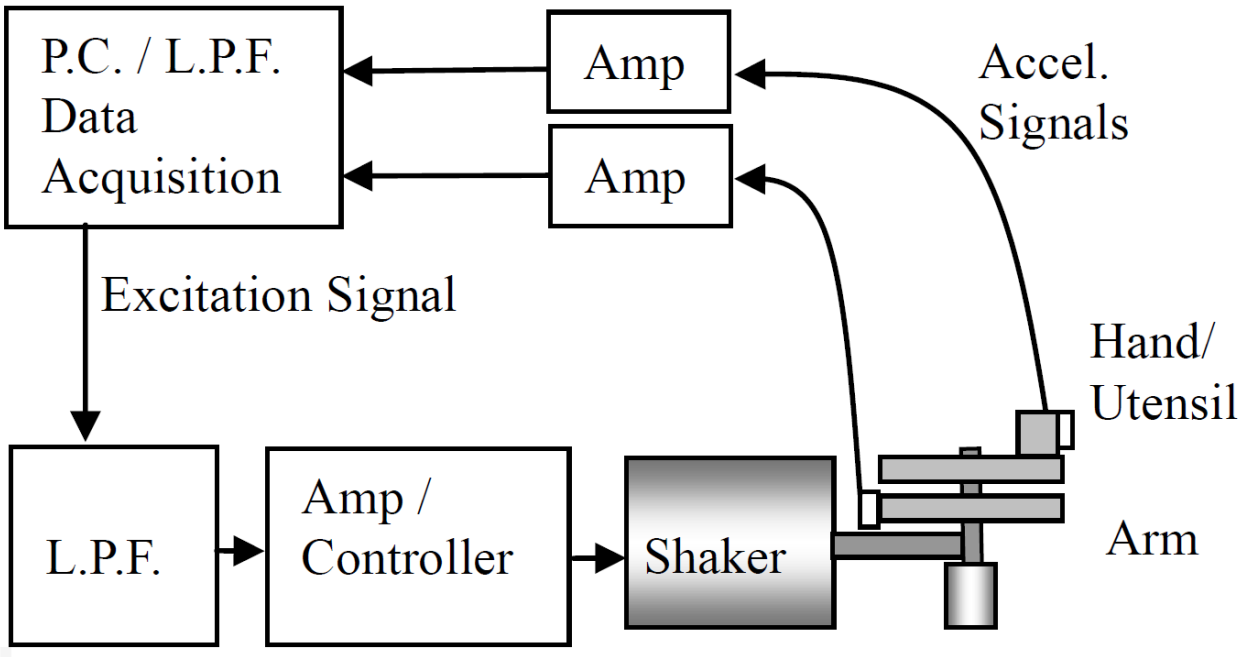

Figure 28: Block diagram of the measurement hardware[24]

The Frequency Response Function of interest is primarily the FRF where the output is the vibration of the object under test and the input is the vibration of the excitation. For the purpose of getting these signals, two accelerometers are mounted at the two points of interest as shown in Figure (28).
Before converting the signals from analogue to digital, the acceleration signals must be amplified, which is achieved using two Model 480C02 Signal Conditioners for ICP Sensors geared to the accelerometers. For the purpose of analog digital converting the output signals of the amplifiers, the module NI 9215 from National Instruments is used. It is a 4 channel ±10V simultaneous analog input having 100kS/s per channel. The two modules NI 9263 and NI 9215 are plugged into the NI cDAQ-9172 USB Data Acquisition System from National Instruments in order to create a connection to the LabVIEW software.

9.2.4 Measurement software

The task of the measurement software is to control the measurement hardware in a way to generate a Frequency Response Function.
A flowchart of this software can be found in the subsequent Figure (29). The boxes marked green are software functions that communicate with the

measurement hardware, either in a writing or reading direction.

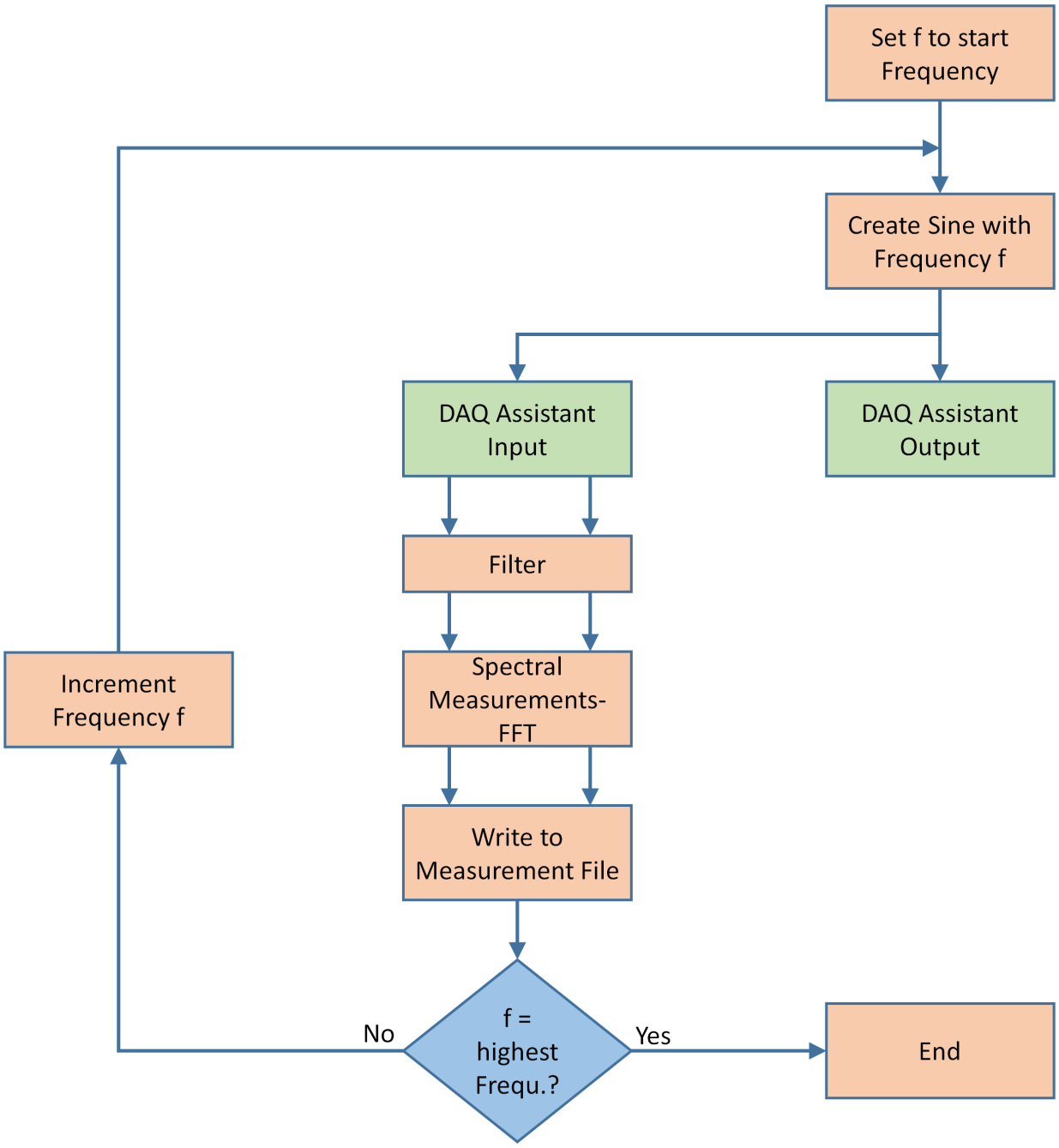

Figure 29: Flowchart of measurement software

The software concept shown in Figure (29) was implemented in LabVIEW, which is a language providing simple functions to communicate with the selected measurement hardware.
The sweep needed for the FRF starts by setting the actual output frequency, labeled as f in Figure (29), to the lowest frequency of interest in the FRF. Next, time values of a sinusoid using this frequency have to be created. These time values are fed into the DAQ Assistant output, which is

configured to communicate appropriately with the analog output module NI 9263. In parallel to each data value output by the DAQ, a data point is collected by the DAQ Assistant input, which is configured properly to receive data from the module NI 9215. Note that the DAQ Assistant input always receives two values in parallel, stemming from each of the amplified accelerometers' signals. In Figure (29), this fact is annotated by using two arrows in parallel.
These two measured signals are filtered to eliminate frequencies of no interest. Afterwards, these two data streams (input and output signal) are processed trough a Fast Fourier Transform (FFT) from the LabVIEW's Measurements Spectral function set. From the spectra of these two streams, the amplitude of the input excitation at the frequency f and also the amplitude of the resulting output vibration can be obtained. These two pieces of information are written to a file using the LabVIEW built-in function Write To Measurement File. After that, the procedure, starting with creating a sinusoid, is repeated with an incremented frequency f.
The execution is stopped if the frequency f reaches the highest frequency of interest in the Frequency Response Function.
Following this, the created file can be exported and the data can be processed with a program that works with numerical values, e.g. MATLAB, in order to create the Frequency Response Function plot.

10 Design Decision and Results

This section is about the parameters for the Parkinson's Assistive device, which are needed for the identified properties of a human arm as discussed in Section (8). As mentioned in Section (7), the developed equations for the translational movement are used for the rotational movement as it yields the same Frequency Response Function.
The following parameters refer to Figure (13) and were obtained in Section (8).

$$m_1 = 0.0009375$$

$$c_1 = 0.0299$$

$$k_1 = 0.7915$$

Using these parameters for the first body in the Two Degrees of Freedom model and using the approximation for the minimum from Equation (16) yields the desired values for the second body. Note that the variable c_2 does not appear in this approximation even though the magnitude of it has an effect on the shape of the FRF plot. A higher damping c_2 yields a broader trough, where a lower damping leads to a sharper trough reaching close to zero.

$$m_2 = 0.001$$

$$c_2 = 0.00125$$

$$k_2 = 0.98646$$

Based on these determined parameters, Frequency Response Function plots can be developed which describe the behavior of the device over the frequency range of interest. The FRF $T_{\frac{X_1}{F_1}}(\omega)$ is of paramount importance as it describes the factor by which an exciting force $F_1(t)$ (which models the tremor excitation) passes through to the output X_1, the human arm. The plot of the FRF $T_{\frac{X_1}{F_1}}(\omega)$ together with the One Degree of Freedom system representing the arm is shown in Figure (30).

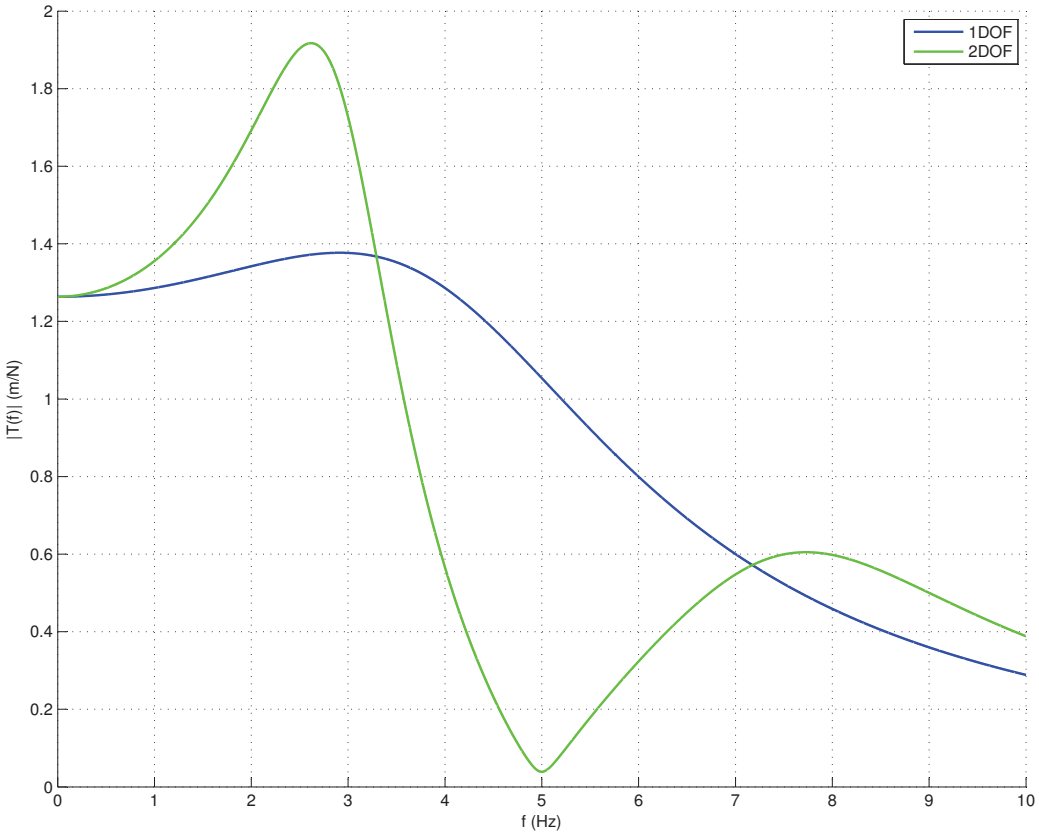

Figure 30: Amplitude of both the 1DOF - $T(\omega)$ and the 2DOF - $T_{\frac{X_1}{F_1}}(\omega)$ systems

The blue plot in Figure (30) shows the original human arm/wrist system modeled as One Degree of Freedom. The green plot line in Figure (30) depicts the final result, i.e. the Parkinson's patient's arm while wearing the device.
Furthermore, Figure (31) shows the Frequency Response Function $T_{\frac{X_1}{F_2}}(\omega)$, which represents the effect that a excitation on the wearable device has on the position of the arm. Figure (32) depicts the FRF $T_{\frac{X_2}{F_1}}(\omega)$ which constitutes the effect that the tremor of the patient's arm has on the position of the wearable device. Lastly, the plot in Figure (33) is of the Frequency Response Function $T_{\frac{X_2}{F_2}}(\omega)$ and expresses the effect that a force acting on the wearable device has on its position.
The plots shown in Figures (30) to (33) were created using the parameters from the current Section (10).
A characteristic value can be obtained comparing the Frequency Response Function of the original system to the FRF of the hand wearing the wearable device, i.e. 1DOF versus 2DOF in Figure (30). Comparing the value

at 5Hz, the frequency of interest, yields a possible reduction of the tremor of about 96 percent at this frequency.

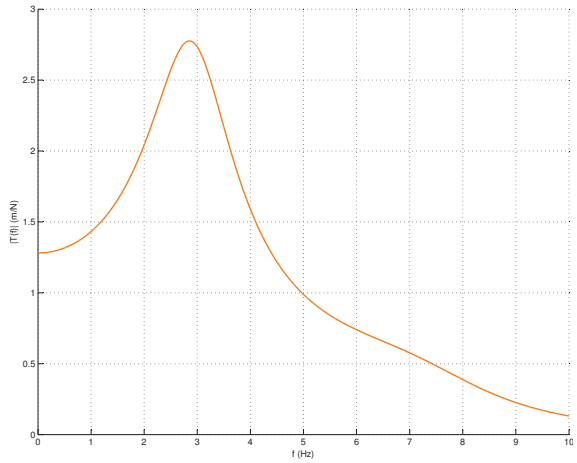

Figure 31: FRF plot of $T_{\frac{X_1}{F_2}}(\omega)$

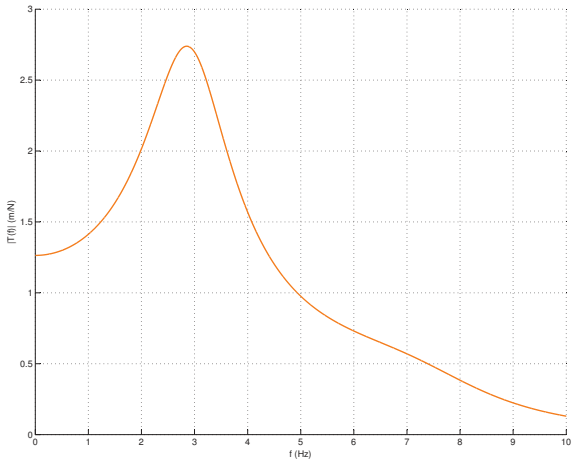

Figure 32: FRF plot of $T_{\frac{X_2}{F_1}}(\omega)$

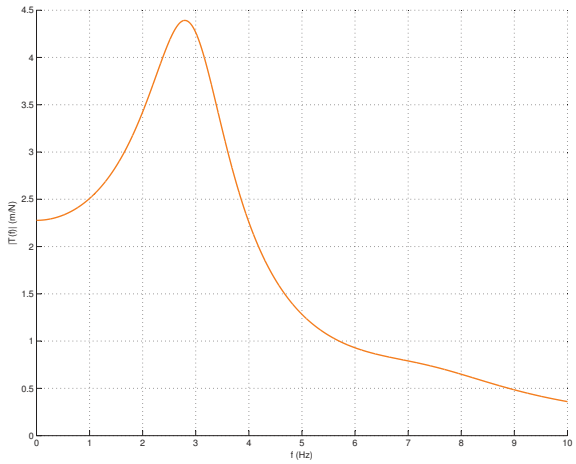

Figure 33: FRF plot of $T_{\frac{X_2}{F_2}}(\omega)$

11 Discussion and Conclusion

During the research period at University of Portland, first the theory around the mathematical model was covered. An exact mechanical implementation of the wearable device was developed and drawn as a SolidWorks model. Since further confidential research is taking place, these drawings cannot be published at this point. Therefore, the significantly more complex system was described in a simplified way using only Two Degrees of Freedom.
Based on this model, calculations lead to a possible reduction of the Parkinson's patient's hand tremor by 96 percent at the excited frequency of 5Hz.

In addition to the theoretical results, the SolidWorks model was used to create a 3D-printed prototype of the wearable device. The next step will be an extensive testing phase using the testing environment described earlier. This phase has just begun and therefore no publishable results are available yet. Further research should also focus on testing the wearable device on human subjects.

The University of Portland is a pioneer in Parkinson's research, and Dr. Timothy Doughty plans to proceed researching in this area. Therefore, the results of this work will contribute to attain results in the development for further technologies to assist Parkinson's disease patients.

References

[1] http://www.pdf.org/symptoms.

[2] David Buckwell Michael Gresty. Spectral analysis of tremor: understanding the results. *Journal of Neurology, Neurosurgery, and Psychiatry*, 53(11):976–981, 1990.

[3] Nicholas Bankus Timothy A. Doughty. Mechanical modeling and design for reduction of parkinsonian hand tremor. *ASME 2010 International Mechanical Engineering Congress and Exposition - Paper No. IMECE2010-39073*, 2:521–527, 2010.

[4] Steven K.Charles Allan W. Peaden. Dynamics of wrist and forearm rotations. *Journal of Biomechanics*, 47(11):2779–2785, 2014.

[5] http://engineering.up.edu/default.aspx?cid=11627&pid=6711.

[6] http://www.pdf.org/en/parkinson_statistics.

[7] http://www.mayoclinic.org/diseases-conditions/parkinsons-disease/basics/definition/con-20028488.

[8] http://aje.oxfordjournals.org/content/157/11/1015/F1.expansion.

[9] https://www.michaeljfox.org/understanding-parkinsons/living-with-pd/topic.php?causes.

[10] http://phys.org/news/2010-10-parkinson-disease-closer.html.

[11] https://www.atrainceu.com/course-module/2455847-146_parkinsons-for-ot-module-01.

[12] http://www.pdf.org/en/causes.

[13] http://www.pdf.org/en/meds_treatments.

[14] M.D. Michael S. Okun. Deep-brain stimulation for parkinson's disease. *The New England Journal of Medicine*, 367(16):1529–1539, 2012.

[15] Singiresu S. Rao. *Mechanical Vibrations (5th Edition)*. Prentice Hall, 2010.

[16] http://morphopedics.wikidot.com/physical-therapy-management-of-colles-fracture.

[17] H.E.J. (DirkJan) Veegerc Mohsen Makhsous Peter Van Roy Carolyn Anglin Jochem Nagels Andrew R. Karduna Kevin McQuade Xuguang Wang Frederick W. Werner Bryan Buchholz Ge Wua, Frans C.T. van der Helm. Isb recommendation on definitions of joint coordinate systems of various joints for the reporting of human joint motion—part ii: shoulder, elbow, wrist and hand. *Journal of Biomechanics*, 38(5):981–992, 2005.

[18] Charles Steven K Drake, Will B. Passive stiffness of coupled wrist and forearm rotations. *Annals of Biomedical Engineering*, 42(9):1853–1918, 2014.

[19] De Leva. Adjustments to zatsiorsky-seluyanov's segment inertia parameters. *Journal of Biomechanics*, 29(9):1223–1252, 1996.

[20] Nagurka M.L. Dolan J.M., Friedman M.B. Dynamic and loaded impedance components in the maintenance of human arm posture. *IEEE Transactions on Systems, Man, and Cybernetics*, 23(3):698–709, 1993.

[21] Kirsch Robert F. Crago Patrick E. Perreault, Eric J. Multijoint dynamics and postural stability of the human arm. *Experimental brain research*, 157(4):507–517, 2004.

[22] Goto K. Ito K. Tsuji T., Morasso P.G. Multijoint dynamics and postural stability of the human arm. *Biological cybernetics*, 72(6):475–485, 1995.

[23] http://onlinelibrary.wiley.com/doi/10.1002/uog.5256/pdf.

[24] Dr. Timothy Doughty. *Unversity of Portland*.

[25] http://mbdynamics.com/assets/datasheets/MODAL50ADataSheet.pdf.